International Journal of Heat and Mass Transfer 111 (2017) 246–265

Contents lists available at ScienceDirect

International Journal of Heat and Mass Transfer

journal homepage: www.elsevier.com/locate/ijhmt

Computational modelling of flash boiling flows: A literature survey

Yixiang Liao *, Dirk Lucas

Helmholtz-Zentrum Dresden-Rossendorf, Institute of Fluid Dynamics, Bautzner Landstr. 400, 01328 Dresden, Germany

ARTICLE INFO

Article history:
Received 15 February 2017
Received in revised form 20 March 2017
Accepted 31 March 2017
Available online 7 April 2017

Keywords:
Flashing flow
Nucleation
Coalescence and breakup
Two-fluid model
Poly-disperse

ABSTRACT

A review of published work on the physics and modelling of flashing flows is presented. The term "flashing" refers to a familiar phase change phenomenon initiated by pressure drop. It has gained a great deal of attention due to various industrial safety concerns. Nevertheless, knowledge about the involved physical processes such as formation and growth of bubbles in superheated liquid, and information for appropriate modelling in practical systems is still far from sufficiency. The present work is aimed to provide a brief but comprehensive overview of available theoretical models for these sub-phenomena as well as general modelling frameworks. This kind of review is necessary and helpful for further understanding and investigation of flashing flows in more detail.

Contents

* Corresponding author.
E-mail address: y.liao@hzdr.de (Y. Liao).

http://dx.doi.org/10.1016/j.ijheatmasstransfer.2017.03.121
0017-9310/

1. Introduction

When liquid is at a temperature above the saturation condition corresponding to its pressure, it is superheated. The attainable superheat has a limit, beyond which phase change (vaporization) will take place and consequently the liquid will drop back to the equilibrium (saturation) status. A liquid can gain its superheat in two different ways: being heated or depressurized, e. g. from state A' to B or from A to B in Fig. 1(a). Vaporization taking place under depressurization conditions is often referred as flashing or cavitation.

The fundamental difference between the terms "flashing" and "cavitation" is the temperature (or pressure) level, at which they are taking place [1]. Cavitation occurs at a relatively low temperature (or pressure), e.g. the region I in Fig. 1(b), where vapour density is low and small superheat is enough to initiate and maintain the vaporization process. Bubble expansion is mainly controlled by mechanical non-equilibrium (pressure difference across the interface) while thermal effects are negligible. In contrast, flashing of hot liquid is more like a boiling process, which is characterized by high thermal non-equilibrium (temperature difference across the interface). In this case, bubble growth rate is limited by interphase heat transfer rate instead of mechanical expansion. This mechanism is relevant in high temperature (or pressure) situations, e.g. the region II in Fig. 1(b). In the reality, mechanical and thermal non-equilibrium exist simultaneously in a depressurization process, while in the numerical analysis one of them is often ignored depending on the temperature (or pressure) level. For example, the assumption of pressure equilibrium at the interface is frequently adopted in the modelling of flashing flow.

In total three types of depressurization can be encountered in a practical fluid system, see Fig. 2 below. In a flowing system, liquid may experience dynamic pressure drop as the channel area increases. A pressure release process happens if the safety valve of a pressurized liquid container is opened, cracks or other failures appear in the container wall. Flashing phase change phenomenon can also take place along a vertical flow path due to the hydrostatic pressure drop (see Fig. 2(c)).

Flashing has a fundamental and decisive presence in many industrial and technical applications or scenarios. As examples one can mention (1) flow through cracks, nozzles, valves and orifices [2,3]; (2) hypothetical loss-of-coolant accidents (LOCA) of pressurized water nuclear reactors or blowdown through a horizontal pipe [4]; (3) flashing-induced instability in natural circulation systems [5–7]; (4) failure of pressurized vessels or pipes containing liquefied hazardous gases [8]; (5) flashing fuel spray atomization in engines [9–12]. Under these circumstances, properties of the flashing flow such as discharge flow rates, vapour generation rate, void holdup as well as two-phase morphology are of key safety and economic importance. All these quantities are substantially influenced by the degree of non-equilibrium. Flashing phenomena can be classified as internal flashing in channels or external flashing such as jet flow, and the liquid can be pure or multi-component. This review work mainly focuses on internal flashing of pure liquids. Park and Lee [13] investigated the internal and external flashing modes in a transparent nozzle, and the work of Zuo et al. [14] focused on the external flashing dynamics. In addition, the level of superheat at flashing inception may influence the vapour generation and expansion scenario.

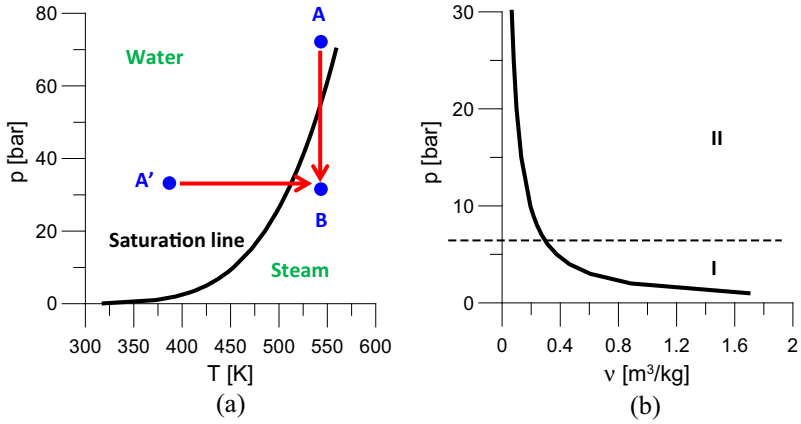

Fig. 1. (a) P-T diagram of saturation water. (b) P-v diagram of saturation steam.

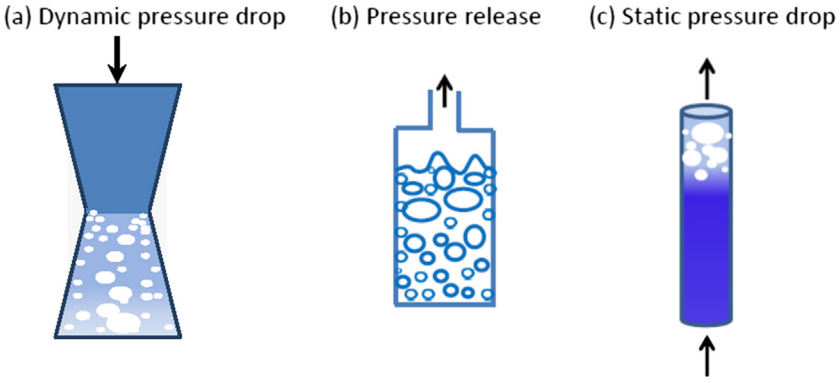

Fig. 2. Various depressurization situations in a fluid system.

Since the middle of last century there have been many theoretical and experimental studies on the two-phase flashing flow owing to great concern about nuclear safety. Nevertheless, in theoretical studies, simplifying empirical assumptions usually have to be adopted due to the complexity of the phenomena. The degree of non-equilibrium is only partially accounted for, or neglected fully. Therefore, the general validity of available methods is largely limited. A comprehensive review on our current knowledge on the flash boiling phenomenon as well as limitations in existing modelling approaches is important for further studies. Review articles on flashing atomization have been published by Sher et al. [15] and Bar-Kohany and Levy [16]. Special attention was given to the quality of spray and the optimization of atomizer. Pinhasi et al. [8] gave an extensive review on the experimental and theoretical study of steady-state critical and blowdown transient pipe flows. The present work aims to extend the review to the state of the art of CFD (Computational Fluid Dynamics) work, since there is a need to develop more accurate and phenomenological models to compliment advances in CFD. In addition, the vast majority of efforts have been conducted on sub-cooled boiling on heated walls, which have to be evaluated or updated for the description of adiabatic flashing flows. The paper is organized as follows. At first, the physics of underlying phenomena as well as corresponding correlations are introduced. Then, existing work on the modelling of flashing two-phase flows is reviewed. Discussion on the necessity and possibility of further improvement completes the paper.

2. Underlying physics and theoretical models

In comparison to single-phase flow or two-phase flow without mass and heat transfer, boiling flow is apparently much more complicated from the physical point of view. One of many challenges is to understand the mechanism of bubble formation in pure liquid and to describe the transition from pure liquid to vapour-liquid mixture, i.e. flashing inception.

2.1. Flashing inception

Flashing inception appears when the superheat limit is reached. The maximum degree of attainable liquid superheat or pressure undershoot determines the intensity of subsequent boiling process and void fraction development. It is therefore important to predict it correctly. There are three definitions for the superheat limit of a practical system. It can be defined theoretically from either thermodynamic principles or kinetic considerations [8]. The thermodynamic limit is the boundary of absolutely instable states. It is called spinodal curve, see Fig. 3(a), within which infinitesimally small fluctuations will inevitably lead to phase separation. For a pure liquid, the thermodynamic limit of superheat is defined by states for which:

$$\left(\frac{\partial P}{\partial V}\right)_T = 0. \tag{1}$$

In principle, the thermodynamic limit can be determined rigorously by using Eq. (1) together with an equation of state. Many researchers have tried this approach such as Reid [17] and Lienhard et al. [18]. The main difficulty encountered here is that no satisfactory equations of state applicable in the superheated liquid (metastable) region exist [8,19].

Furthermore, Eq. (1) defines only a fictional limit that could never be verified experimentally, because the liquid always begins to flash before it reaches this limit. Therefore, it is often replaced by an empirical kinetic homogeneous nucleation limit, which can be observed experimentally. Lienhard and Karimi [12,20] have shown that the two limits lie very close to each other, see Fig. 3(b).

However, the homogeneous nucleation limit can only be reached under carefully controlled laboratory conditions, e.g. pure substance, perfectly clean vessels and no wall effects. In most practical circumstances these ideal conditions cannot be met and the metastable liquid will undergo phase change before it reaches the homogeneous nucleation limit. In this case, nucleation occurs around pre-existing nuclei or gaseous seeds such as dissolved foreign gases or poorly wettable cavities on solid surfaces, which are distributed randomly and non-uniformly. This flashing inception mechanism is called heterogeneous nucleation. The threshold determined by the heterogeneous nucleation is symbolically represented by the red dash line in Fig. 3(b), which is much lower than the homogeneous one. Therefore, only heterogeneous nucleation is discussed in the modelling part below.

2.2. Nucleation modelling

Bubble number density is one of the most important parameters in bubbly two-phase flow systems, since it determines the mean bubble size and the interfacial area concentration. Nucleation is one of the phenomena that affect the budget of bubble number density. The nucleation process is often depicted in three ways, i.e. by homogeneous "seeding", a "step" function or additional "nucleation" models, see Fig. 4(a)–(c).

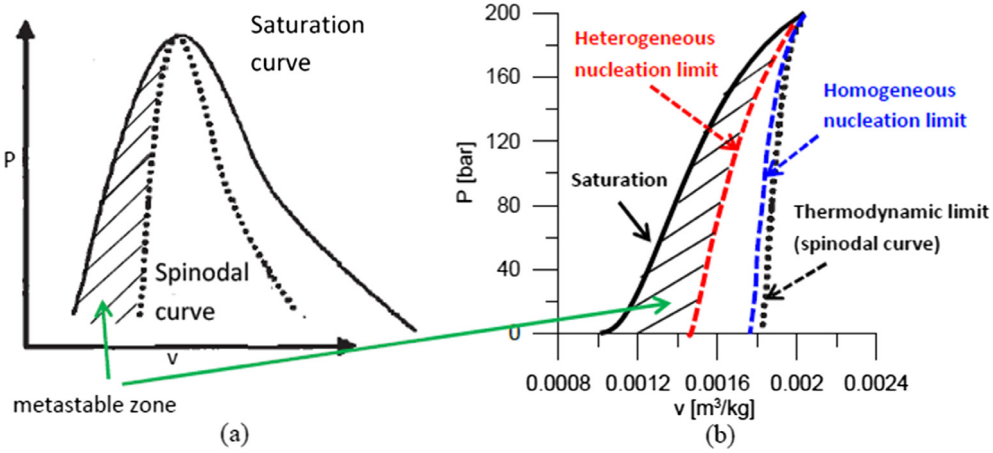

Fig. 3. Spinodal curve and attainable superheat limit of water.

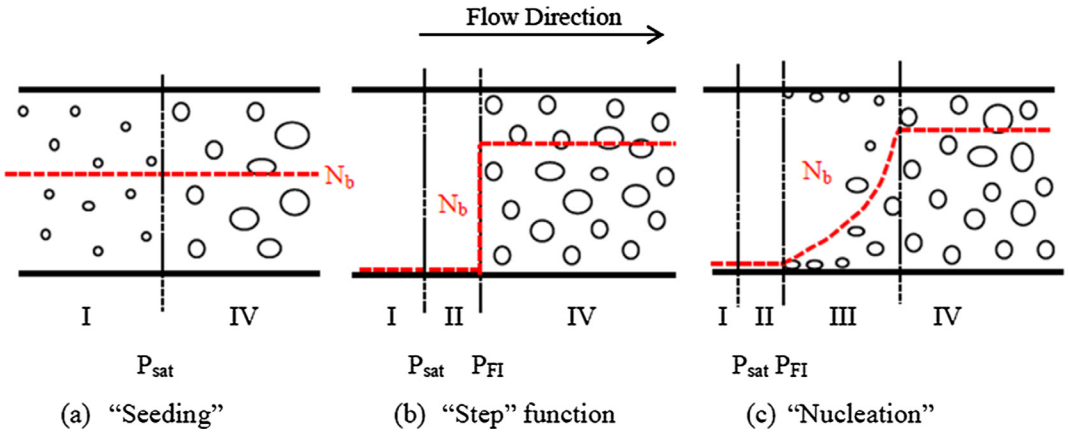

Fig. 4. Approaches used for modelling of the nucleation process.

Along the flow direction, four zones can be distinguished:

Zone I: sub-cooled liquid
Zone II: superheated liquid (metastable)
Zone III: nucleation (non-equilibrium)
Zone IV: equilibrium

The Zone II/Zone III and Zone III are neglected in the modelling approaches of (a) and (b), respectively.

2.2.1. Homogeneous "Seeding"

It is assumed that sub-cooled liquid is "seeded" homogeneously with a certain number of tiny vapour bubbles (see Fig. 4(a)). They will start to grow as soon as the liquid becomes "saturated" ($P = P_{sat}(T_0)$) and correspondingly vapour volume fraction starts to increase as a result of phase change. The mean bubble diameter increases according to the following relation:

$$d_b = \left(\frac{6\alpha}{\pi N_b}\right)^{1/3}, \tag{2}$$

where α is the vapour volume fraction and N_b is the number concentration of bubbles.

This method avoids modelling the stochastic distribution and activation of nucleation sites. Due to the simplicity it has often been adopted in the modelling of flashing flows. For example, a value of $N_b = 10^9$–10^{11} m^{-3} has been used by several authors [21–24] for the critical flow problem of water-steam mixtures, while Laurien [25] assumed $N_b = 2 \times 10^6$ m^{-3} for the CFD simulation of flashing phenomena in pipe elbows. The value was found to be strongly affected by the initial liquid temperature [8]. It is worth noting that an equivalent method by prescribing the bubble diameter d_b instead of N_b has been more frequently employed [26–28]. In spite of that fact Laurien [25] suggested that the former is more close to the physical picture of flashing or boiling phenomena, since it allows bubbles to grow.

Besides a strong dependence of the results on the presumed N_b (or d_b), one major limitation of the method is that it is incapable of capturing the metastable and non-equilibrium stages, namely the zone II and zone III. On the other hand, the width of the metastable zone has been shown to have a significant effect on the intensity of subsequent boiling, since it determines the maximum superheat degree at flashing inception.

2.2.2. "Step" function

The second method attempts to determine the low border of the metastable zone, i.e. the nucleation limit (see Fig. 3(b)), by introducing an empirical correlation for the flashing inception pressure P_{FI}. As the superheat threshold is reached, bubble number density increases rapidly from a negligibly low value to a maximum value by assuming that almost all nucleation sites are activated at this moment. The flow develops suddenly from single-phase to homogeneous two-phase. In other words, nucleation takes place only in a quite narrow zone, which can be treated as a point/line/surface respectively in a 1D/2D/3D case. This treatment is obviously too arbitrary, since it is not clear how wide is the nucleation zone in a certain flashing flow [29]. Furthermore, it should be case-dependent, e.g. depending on surface conditions, liquid properties, depressurization rate, and so on.

Based on the classical homogeneous nucleation theory [30,31], a semi-empirical correlation for the pressure-undershoot (P_{sat}-P_{FI}) was derived by Alamgir and Lienhard [32].

$$\Delta P_{FI} = P_{sat} - P_{FI} = \left[\frac{16\pi\sigma^3}{3k_B T_c (1 - \upsilon_l/\upsilon_g)^2 \left(\frac{Gb}{\varphi}\right)}\right]^{1/2}, \tag{3}$$

where k_B, T_c, υ_l, υ_g, Gb, φ are Boltzmann constant, critical temperature, liquid and vapour specific volume, Gibbs number and heterogeneity factor, respectively. The ratio of Gb/φ at the flashing inception position is obtained empirically:

$$\frac{Gb}{\varphi} = \frac{28.2 \pm 5.8}{0.1058 T_r^{28.46} \cdot (1 + 14\Sigma'^{0.8})}, \tag{4}$$

where $T_r = T_i/T_c$ is the relative temperature and Σ' is the static depressurization rate. The data used to derive the correlation are in the range:

$$0.62 \leqslant T_r \leqslant 0.935,\ 405.3\ \text{MPa/s} \leqslant \Sigma' \leqslant 1.82689 \times 10^5\ \text{MPa/s}.$$

The Alamgir and Lienhard correlation has been widely adopted [29,33–36] and successfully modelled transients with high depressurization rates and stagnation conditions. It was extended by Abuaf et al. [33] and Jones [37] to flowing systems by considering the convective and turbulence effects. Schrock and his co-workers [36,38,39] modified the correlation by introducing a multiplication factor, which was correlated in terms of Reynolds number and subcooling Jakob number. According to Lee and Schrock [39] the fact that the modification factor has a value significantly less than unity indicates an important role of heterogeneous nucleation in wall cavities in addition to homogeneous nucleation. Finally, they proposed a cavity flooding incipient flashing model. A slightly modified relation was developed by Levy and Abdollahian [40] based upon the experimental data of Reocreux [41] and Wu and Zimmer [42] for nozzle flow.

A further empirical correlation was developed by Barták [43] and later employed in Tiselj and Petelin [44], which has the same form as Eq. (3) with the exception of

$$\frac{Gb}{\varphi} = 10^{(11-0.0274T_0)} \cdot 36\Sigma'^{-0.37}, \tag{5}$$

and the initial temperature T_0 instead of the critical one T_c.

It is valid for the range:

$$100 \leqslant T_0 \leqslant 300\ ^\circ\mathrm{C},\ 400\ \mathrm{MPa/s} \leqslant \Sigma' \leqslant 2\times 10^5\ \mathrm{MPa/s}.$$

Elias and Chambré [45] presented a theoretical model for the maximum pressure undershoot based on asymptotic analysis of the mass and energy equations at the flashing inception point.

$$\left(\frac{4\Sigma'}{\sqrt{\pi}P_{sat}}\right)^4 \frac{1}{3\beta V_M C_0}\left[\frac{3c}{A(\theta_m)\theta_m^3}\right]^3 = \frac{e^{-c\varphi/\theta_m^2}}{\varphi^3}, \tag{6}$$

where V_M is the volume of a vapour molecule.

The model was shown to be applicable for both static and flow systems, low and high decompression rates. At low decompression rates, the heterogeneity effect becomes significant, which is reduced with an increase in decompression rate.

The normalized pressure-undershoot is defined as:

$$\theta_m = \frac{P_{sat} - P_{FI}}{P_{sat}}. \tag{7}$$

The coefficient c is given by

$$c = \frac{16\pi\sigma^3}{3T_0P_{sat}^2\left(1-\rho_g/\rho_l\right)^2}, \tag{8}$$

and β by

$$\beta = \frac{a_h\rho_g h_{lg} + \rho_l(\rho_l - \rho_g)}{P_{sat}(a_h + \rho_l a_P)^2}, \tag{9}$$

where a_h and a_P are the partial derivatives of the liquid density with respect to enthalpy and pressure, respectively.

The function $A(\theta)$ is defined as

$$A(\theta) = \left(\frac{3V_M}{4\pi}\right)^{2/3} \frac{4\pi\rho_g P_{sat}\theta}{\rho_l\sqrt{2\pi m_W k_B T_0}}. \tag{10}$$

According to Eq. (6) the pressure undershoot is a function of three independent variables, T_0, Σ' and the heterogeneity factor φ. An empirical correlation for φ was derived from experimental data for various liquid temperature and decompression rates.

Nevertheless, the premise for the application of above models is that both the local real pressure and the saturation pressure corresponding to liquid temperature have to be known. That means that either the saturation pressure is assumed constant spatially and temporally, or the functional dependence of saturation pressure on local temperature is implemented.

Furthermore, the pressure-undershoot can be transformed approximately to liquid superheat through the linearized Clausius - Clapeyron equation

$$P_{sat}(T_{FI}) - P_{FI} = (T_{FI} - T_{sat}(P_{FI})) \cdot \frac{h_{lg}}{T_{sat}(P_{FI})\left(1/\rho_{g,sat} - 1/\rho_{l,sat}\right)}. \tag{11}$$

2.2.3. "Nucleation" model

The last method attempts to describe the non-equilibrium nucleation zone by introducing a nucleation model, see Fig. 4(c). It is most close to the physical picture, but needs reliable constitutive relations. Three types of nucleation mechanisms are present in a flashing process: bulk homogeneous, bulk heterogeneous and wall nucleation. As mentioned previously, homogeneous nucleation occurs at a much higher superheat level than that observed in experiments (see Fig. 3). In the following, attention is paid to heterogeneous nucleation models including bulk and wall.

2.2.3.1. Bulk heterogeneous nucleation. In general, there are two kinds of models for the description of this mechanism. The most popular one is to modify the classical homogeneous nucleation theory, and the other one is to presume a Probability Density Function (PDF) of nuclei in the bulk.

2.2.3.1.1. Modified homogeneous nucleation models. It is believed that heterogeneous nucleation in a flashing process is of the same nature as homogeneous volumetric nucleation [32,46]. Both of them are triggered by local thermodynamic state fluctuations, but the onset of nucleation in the flashing process occurs within the near-wall liquid volume. Due to the intervention of the walls, the activation energy for the nucleation sites is much lower. According to this theory, the nucleation rate per unit volume can be computed based on the classical theory, i.e.

$$J_{het,B} = J_0 \cdot \exp(-Gb) = J_0 \cdot \exp\left(-\frac{W_{cr}\cdot\varphi}{k_B T_0}\right), \tag{12}$$

wherein parameters J_0, W_{cr} are nucleation site density and critical work required to create a vapour bubble of the critical size, respectively. The heterogeneity (or work reduction) factor φ is smaller than unity. Empirical correlations relating φ with other relevant parameters such as liquid temperature and rate of depressurization were proposed by some researchers, e.g. Alamgir and Lienhard [32], Elias and Chambré [45]. In contrast, φ is treated directly as an overall adjustable constant in the work of Valero and Parra [47] and Rohatgi and Reshotko [48].

For single component systems, the energy barrier for nucleation is often postulated as the energy that must be deposited in the body of the pure liquid in order to create a nucleus of the critical size, R_{cr}. It arises from the bulk and the surface contributions. The bulk term refers to the work consumption for displacing the liquid, which is always negative. The surface term is energy stored in the surface of the bubble. Consequently, the critical work is given by

$$W_{cr} = 4\pi R_{cr}^2\sigma - \frac{4}{3}\pi R_{cr}^3\Delta P_{cr} = \frac{4}{3}\pi R_{cr}^2\sigma. \tag{13}$$

In the derivation of Eq. (13) it is assumed that the critical nucleus is always in thermodynamic equilibrium with its surrounding superheated liquid, and the vapour density is much smaller than the liquid one. Extensions to consider "molecular" work for non-equilibrium states and "crowed" state effect are discussed in Skripov [46].

The critical size for a bubble to grow continuously in superheated liquid is

$$R_{cr} = \frac{2\sigma}{[P_{sat}(T_0) - P_l]\left(1-\rho_{g,sat}/\rho_{l,sat}\right)}. \tag{14}$$

Since liquid superheat instead of pressure undershoot is used frequently for the characterizing of the flashing process, Eq. (14) is often reformulated by applying the linearized Clausius-Clapeyron equation.

$$R_{cr} = \frac{2\sigma T_{sat}}{(T_0 - T_{sat})h_{lg}\left(1-\rho_{g,sat}/\rho_{l,sat}\right)}\left(\frac{1}{\rho_{g,sat}} - \frac{1}{\rho_{l,sat}}\right). \tag{15}$$

When $\rho_{g,sat} << \rho_{l,sat}$, it is simplified as:

$$R_{cr} = \frac{2\sigma T_{sat}}{(T_0 - T_{sat})h_{lg}\rho_{g,sat}}. \tag{15'}$$

The exponential term in Eq. (12) is universal, which has been retained in all subsequent models in this category. The major difference between various theories lies in the evaluation of the pre-exponential factor J_0. The general form for the factor J_0 is [8]

$$J_0 = N_s B'. \tag{16}$$

Herein N_s is the effective number density of heterogeneous nucleation sites, which is not completely determined and may also depend on the contact angle between liquid and solid impurities. However, for simplicity, N_s is often assumed to be equal to the number density of liquid molecules, N_M, and not affected by the heterogeneity [47,49]. On the other hand, in the work of Rohatgi and Reshotko [48] and Ardron [50] this parameter was treated as an adjustable constant. In principle, the heterogeneous nucleation rate of combined processes such as dissolved gases and solid impurities can be described provided a suitable choice of N_s and φ is made.

For the determination of the rate of molecular interactions, B', the simple Döring-Volmer formula [30,3] is well-accepted

$$B' = \sqrt{\frac{2\sigma}{\pi m_W B}}, \tag{17}$$

where m_W is the mass of a single molecule, and the coefficient B is given by

$$B = \frac{1}{3}(2 + P_l/P_{sat}). \tag{18}$$

As the value of P_l/P_{sat} varies from 0 (thermal equilibrium) to 1 (mechanical equilibrium), B will change from 2/3 to 1. According to Blander and Katz [51], it is usually equal to 2/3, but for cavitation $B = 1$. Note that in the derivation of Eq. (17) neither hydrodynamic nor transport effects on bubble nucleation are included. Corrections accounting for the effects of heat and diffusion as well as viscous and inertial forces have been proposed by Kagan [52], Skripov [46] and many other authors. For example, in Kagan's analysis, the rate of nucleation is constrained by the heat transfer from the bulk liquid to the interface. More recent alterations of the basic theories are to include non-Newtonian effects, e. g. for use specifically with polymeric systems [53]. A good review on nucleation theory is given by DeBenedetti [54].

According to Riznic et al. [55], the heterogeneous theory based on Eq. (12) yields extremely high liquid superheats for water, especially at lower pressure. The possible reason as stated by Skripov [46] is that the classical theory itself is not applicable to water at $P < 0.5\ P_{cr}$.

2.2.3.1.2. Presumed PDF function. A novel method based on statistical theory was presented in Kumzerova and Schmidt [56]. It is supposed that bubbles formed on nucleation sites in the bulk have a normal size distribution, i.e.

$$n_b(r, r_{\max}, \vartheta) = \frac{N_s}{\sqrt{2\pi\vartheta^2}} \exp\left(-\frac{(r - r_{\max})^2}{2\vartheta^2}\right). \tag{19}$$

Herein ϑ is the standard deviation and r the nucleation site radius. The maximum radius of the normal distribution, $r_{\max}$, is assumed to be the critical radius corresponding to the flashing inception pressure:

$$r_{\max} = \frac{2\sigma}{P_{sat} - P_{FI}}. \tag{20}$$

The total number density of sites, $N_s = 10^8\ \mathrm{m}^{-3}$ and $\vartheta = 0.5$ was used by the authors.

Finally, the bubble density at the certain moment of time generated by nucleation is obtained from the shaded area under the distribution curve, see Fig. 5.

The critical bubble size is given by Eq. (14) or Eq. (15).

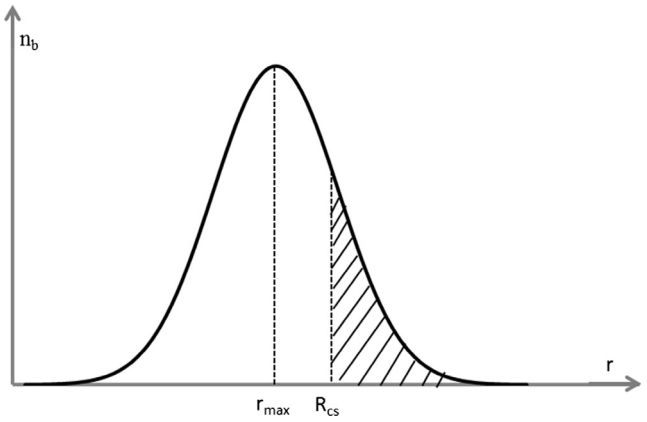

Fig. 5. Normal size distribution of the nucleation sites.

2.2.3.2. Wall nucleation. Besides bulk nucleation, nucleation on the vessel wall is acknowledged as a predominant source of bubbles even under adiabatic wall conditions. The relative importance of the two mechanisms depends on the wall features, liquid properties, pressure level as well as depressurization rate. Models have been developed for both smooth and non-smooth solid walls.

2.2.3.2.1. Smooth wall. A well-accepted model was proposed by Blander and Katz [51], which is a modification of the bulk homogeneous nucleation expressed in Eq. (12):

$$J_{het,W} = N_s^{2/3} \cdot S \cdot \sqrt{\frac{2\sigma}{\pi m_W B\varphi}} \cdot \exp\left(-\frac{W_{cr}\varphi}{k_B T_l}\right), \tag{21}$$

where S is a geometrical factor $0.5(1 + \cos\theta)$, and θ is the contact angle between liquid and solid wall. The exponent 2/3 of N_s is introduced to consider number density of liquid molecules at the surface instead of in the volume. The heterogeneity factor φ is:

$$\varphi = \frac{1}{4}(2 + 3\cos\theta - \cos^3\theta). \tag{22}$$

Note that the parameter S in Eq. (21) decreases while the square root and exponential term increases as the contact angle θ increases. In addition, as pointed out by Deligiannis and Cleaver [57], it is hardly possible to specify a priori for θ even for most ideal conditions. The agreement with experiments depends on careful choice of the parameter.

Furthermore, the model was found to create large numerical instabilities by Marsh and O'Mahony [58] in their CFD simulation of nozzle critical flow and flashing slurry applications. Possible explanations may be the fundamental simplifications made in the computation of the energy barrier discussed in the last subsection. Consequently, they had to modify the correlation as:

$$J_{het,W} = N_s^{2/3} S \sqrt{\frac{2\sigma}{\pi m_W B}} \cdot \exp\left(-\frac{\varphi'}{(T_{sat} - T_l)^n}\right), \tag{23}$$

with two new adjustable parameters φ' and n.

In summary, the predictive ability of above models is limited greatly by the uncertainty in the choice of nucleation site density, N_s, heterogeneity factor, φ, or the contact angle θ. In most cases, the value of the heterogeneity factor is found to be significantly less than unity, e.g. $\varphi = 5 \times 10^{-6}$ by Rohatgi and Reshotko [48] and $\varphi = 0.055$ to 2×10^{-7} by Alamgir and Lienhard [32]. It implies that the true physics of nucleation is gas/vapour trapped in wall cavities rather than molecular fluctuations in the superheated liquid [59].

2.2.3.2.2. Non-smooth wall. Kottowski [60] tried to describe cavity nucleation on non-smooth wall by using the Blander and Katz [51] model, but with a modified heterogeneity factor:

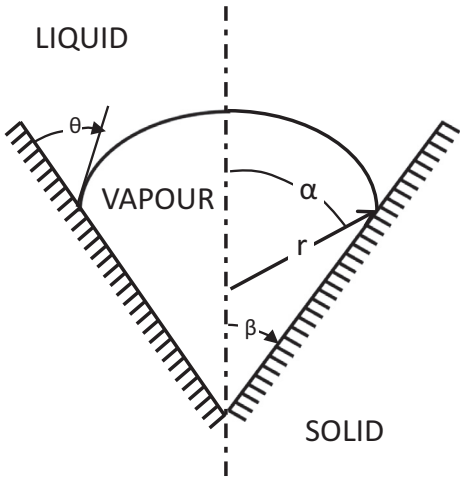

Fig. 6. Vapour embryo in a conical cavity at heated and adiabatic wall [61].

$$\varphi = \frac{1}{4}\left(2 - 3\sin(\theta-\beta) + \sin^3(\theta-\beta)\right), \tag{24}$$

where β is the half angle of the cavity, see Fig. 6.

However, the more general way is to make an analogy to nucleation on heated walls. Since the mid of last century numerous experimental and theoretical efforts have been invested in the study of nucleation in cavities on heated walls [62–68]. According to Riznic [55] these correlations in principle can be generalized for adiabatic flashing flow if an appropriate superheat is introduced. The argument was supported by Kolev [69], who insisted that boiling and adiabatic flashing be driven by the same physics. For a vapour embryo captured in a conical cavity at the heated wall, energy required for its growth comes from the hot wall, i.e. the effective superheat $T_{sup} = T_W - T_{sat}$. In contrast, for the adiabatic case, the wall and vapour embryo is often assumed in thermal equilibrium. The growth of vapour embryo is kept mainly by heat infusion from surrounding liquid, therefore $T_{sup} = T_L - T_{sat}$. The liquid temperature profile in case of boiling and flashing is sketched in Fig. 7(a) and (b), respectively.

Three representative models have been proposed or modified for the application to flashing systems.

(a) **Riznic model**

In his 1D analysis Riznic et al. [55] extended the relation of Kocamustafaogullari and Ishii [66] for boiling to flashing conditions. Satisfactory agreements were obtained for two steady-state experiments of critical flow in nozzles [41,71].

The nucleation rate per unit area of the wall is computed as:

$$J_{het,W} = N_a \cdot f, \tag{25}$$

where N_a is the activated nucleation site density per unit area on the wall, and f is the frequency of bubbles departing from their nucleation sites.

The activated nucleation site density is expressed as follows:

$$N_a = 0.002244 D_d^{2.4}\left\{\frac{\sigma T_{sat}}{(T_l - T_{sat})\rho_g h_{lg}}\right\}^{-4.4}\Psi(\rho^*). \tag{26}$$

It is worth mentioning that the Eq. (23) in original paper is erroneous, which can be easily judged from dimensional analysis.

The property function Ψ is correlated in terms of the density ratio as

$$\Psi(\rho^*) = 2.157\times10^{-7}\left(\frac{\Delta\rho}{\rho_g}\right)^{-3.12}\left(1 + 0.0049\frac{\Delta\rho}{\rho_g}\right)^{4.13}. \tag{27}$$

The bubble departure diameter D_d is calculated based on the modified Fritz equation [72]

$$D_d = 2.64\times10^{-5}\theta\left(\frac{\Delta\rho}{\rho_g}\right)^{0.9}\left(\frac{\sigma}{g\Delta\rho}\right)^{0.5}, \tag{28}$$

where θ is the contact angle in degrees (see Fig. 6).

The departure frequency f is estimated by using the expression given by Zuber [73]:

$$f = 1.18\left(\frac{\sigma g\Delta\rho}{\rho_l^2}\right)^{0.25}\frac{1}{D_d}. \tag{29}$$

As one can see, the bubble departure diameter and frequency depends on the contact angle and properties, while N_a additionally on the degree of superheat, $\Delta T = T_l - T_{sat}$.

From Fig. 8 one can see that the departure diameter and activated nucleation site density increases with an increase in the contact angle θ while the departure frequency decreases. Both departure diameter and frequency decrease as the pressure level is enhanced. However, the activated nucleation site density increases with both pressure level and superheat degree.

(b) **Kolev model**

Kolev [69] calculated the nucleation rate at the wall by considering the heat transfer between superheated liquid in the bulk and the liquid in the boundary layer.

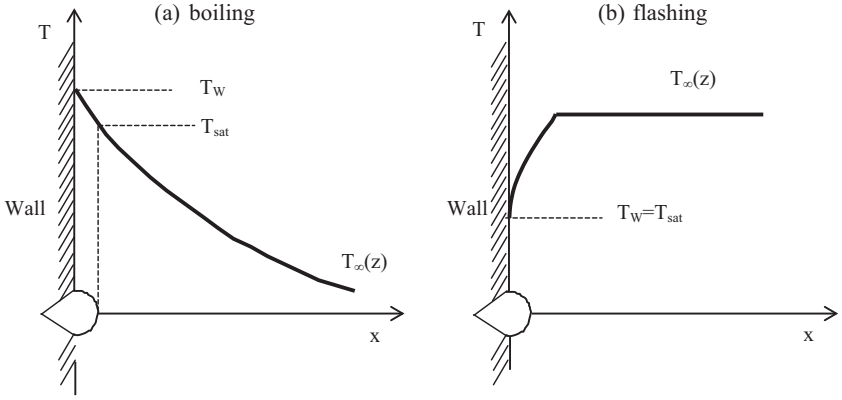

Fig. 7. Temperature profile in boiling and flashing [70].

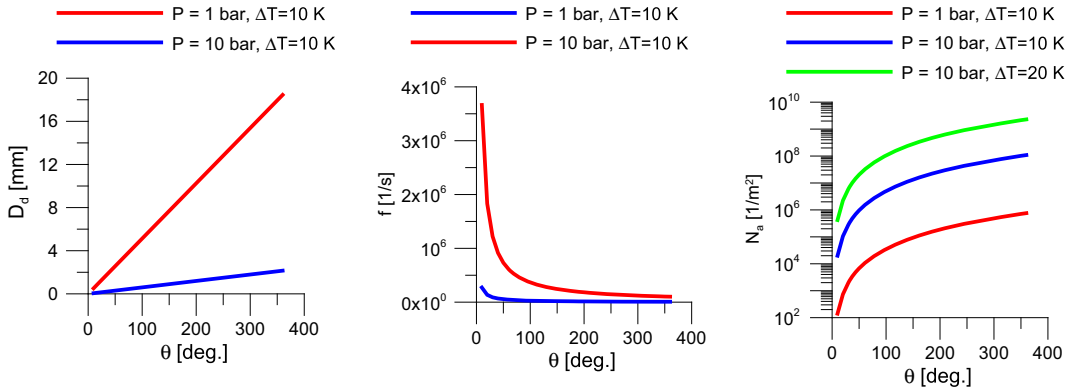

Fig. 8. Bubble departure diameter, frequency and activated nucleation site density predicted by the Riznic model.

Nucleation rate per unit surface area is computed from

$$J_{het,W} = \frac{6\Gamma_W}{\rho_g \pi D_d^3}, \tag{30}$$

where Γ_W is the vapour generation rate on the wall. It is determined by the heat flux from liquid to the wall,

$$\Gamma_W = \frac{\dot{q}}{h_{lg}}. \tag{31}$$

The heat transfer from superheated liquid to the wall is caused by boundary layer turbulence due to bubble growth and departure.

(c) **Jones model**

Unlike Riznic et al. [55] and Kolev [69], Shin and Jones [70] argued that nucleation in sub-cooled wall boiling and in flashing has different nature and requires separate considerations. The correlation of Kocamustafagullari and Ishii [66] for subcooled boiling was found to under-predict the nucleation rate in flashing systems by Jones and Shin [74]. They proposed novel relations for activated nucleation site density, departure frequency and size [75].

The nucleation rate is then calculated according to Eq. (25), and the activated nucleation site density is given by an empirical correlation:

$$N_a = 0.25 \times 10^{-7} \frac{R_d^2}{R_{cr}^4}, \tag{32}$$

The critical radius is estimated by using Eq. (15′) and the departure radius of a bubble is calculated by balancing drag and surface tension forces:

$$R_d = \sqrt{\frac{\mu_l}{\tau_W}\sqrt{\frac{4\sigma R_{cr}}{C_d \rho_l}}}, \tag{33}$$

By approximating the near wall drag coefficient with the Blasius correlation, Blinkov et al. [75] obtained the following correlation for pipe flow

$$R_d = 0.58K^{5/7}\left[\left(\frac{\sigma R_{cr}}{\rho_l}\right)^{1/2}\left(\frac{\mu_l}{\tau_W}\right)^{7/10}\left(\frac{\rho_l}{\mu_l}\right)^{3/10}\right]^{5/7}, \tag{33′}$$

where τ_W is the wall shear stress. The coefficient K was introduced to consider the decrease in drag due to the non-sphericity of the departing bubble but it was taken as unity in all calculations by the authors.

The nucleation departure frequency is estimated by

$$f = C_{dp} \cdot (T_l - T_{sat})^3, \tag{34}$$

where the constant $C_{dp} = 10^4$ [K^{-3} s^{-1}].

Recently, the Jones model was often adopted in CFD work such as [56,76]. Mimouni et al. [77] suggested that their modification for nucleation site density has a generalized formulation:

$$N_{a,mimouni} = \sqrt{210(T_l - T_{sat})^{1.8} N_{a,jones}}, \tag{35}$$

The dependence of nucleation parameters provided by the Jones model on the pressure level, superheat degree and wall shear stress is shown in Fig. 9. One can see that under the same pressure and temperature conditions, the departure diameter and nucleation site density are clearly smaller in comparison to those obtained in the Riznic model (see Fig. 8). In addition, both D_d and

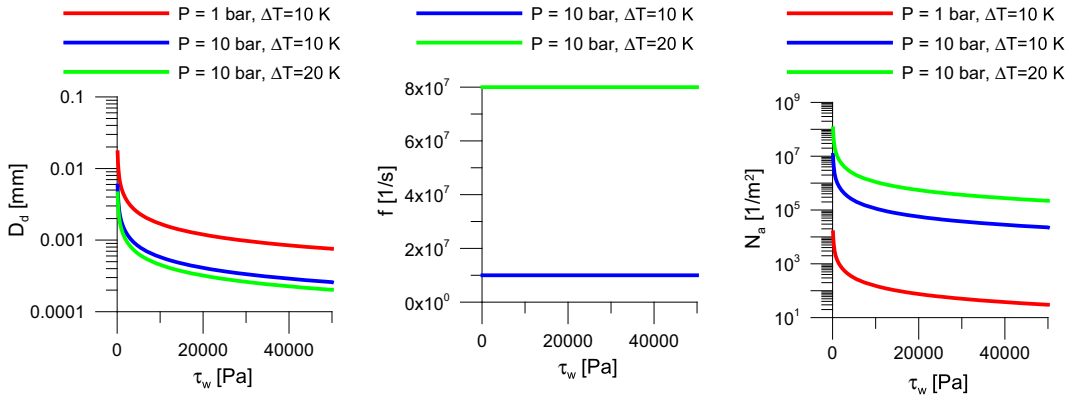

Fig. 9. Bubble departure diameter, frequency and activated nucleation site density predicted by the Jones model.

N_a decrease with an increase in the wall shear stress. Either increasing the pressure or the superheat will lead to a decrease in D_d but an increase in N_a.

In overall, both the quantitative and qualitative performance of the existing nucleation models deviates from each other substantially. In addition, most models were derived originally for one-dimensional applications. The nucleation flux on the wall is often needed to be transformed to a volumetric source in the bulk by multiplying the ratio of the perimeter, ξ, to the cross-sectional area of the pipe, S_p, i.e.

$$J_{het,B} = J_{het,W} \cdot \frac{\xi}{S_p}. \tag{36}$$

However, in a three-dimensional simulation, the transformation should be done by means of multiplication by the ratio between the surface and volume of the control volume closest to the bubble departure position [78], e.g. the wall.

2.3. Bubble growth

The growth of a spherical bubble in an infinite body of superheated liquid is governed by the well-known Rayleigh-Plesset equation. Its general form is written as:

$$\frac{P_b(T_b) - P_\infty(t)}{\rho_l} = R_b \frac{d^2R_b}{dt^2} + \frac{3}{2}\left(\frac{dR_b}{dt}\right)^2 + \frac{4\nu_l}{R_b}\frac{dR_b}{dt} + \frac{2\sigma}{\rho_l R_b}, \tag{37}$$

where P_b is the pressure within the bubble and P_∞ is the external pressure infinitely far from the bubble. In the derivation of Eq. (37), spherical symmetry, constant liquid density ρ_l and viscosity ν_l and uniform pressure P_b and temperature T_b within the bubble are assumed.

By disregarding the surface tension and viscosity terms on the right hand side, Eq. (37) can be simplified as

$$\frac{dR_b}{dt} = \sqrt{\frac{2}{3}\frac{P_b(T_b) - P_\infty(t)}{\rho_l}}. \tag{38}$$

If the cooling effect due to evaporation can be neglected and vapour inside the bubble is assumed at saturation, we have $T_b = T_\infty$ = constant and $P_b(T_b) = P_{sat}(T_\infty)$ = constant. In this case, the bubble growth rate is only dependent on the initial temperature and the pressure undershoot $P_{sat}(T_\infty)$–$P_\infty(t)$. This kind of bubble dynamics is termed "inertia controlled" bubble growth to distinguish it from the "thermal controlled" discussed below. It is the basis of all existing cavitation models.

Nevertheless, in most circumstances the bulk temperature decreases continuously due to the cooling effect of evaporation. If the duration of the process is not extremely short (e.g. ~μs), the temperature difference (T_b–T_∞) will become significant, and determines the rate of bubble growth together with the mechanical tension $P_b(T_b)$–$P_\infty(t)$. The temperature distribution in the liquid has to be evaluated based on the energy balance, which relates the rate of bubble growth or vapour generation to the heat flux at the vapour-liquid interface, i.e.

$$\frac{dR_b}{dt} = \frac{1}{\rho_g A_b}\frac{dm_b}{dt} = \frac{\dot{q}}{\rho_g L} \tag{39}$$

where m_b, A_b is the mass and surface area of the bubble, L latent heat, $\dot{q}$ heat flux supplied to the interface from surrounding liquid and internal vapour. Generally, the nonlinear interphase heat transfer problem can only be solved numerically. Nevertheless, for some special cases analytical solutions can be derived. One well-known example is the asymptotic solution obtained by Plesset and Zwick [79], Forster and Zuber [80], Scriven [81] and others.

$$\frac{dR_b}{dt} = \sqrt{\frac{3}{\pi}}\frac{\rho_l C_P(T_\infty - T_{sat})}{\rho_g L}\sqrt{\frac{a_l}{t}}. \tag{40}$$

It is derived based on following simplifying assumptions:

(i) quiescent liquid, i.e. translational motion between bubble and surrounding liquid equal to zero, no convection
(ii) constant pressure field, i.e. $T_b = T_{sat}$ constant
(iii) isothermal, uniformly superheated liquid of infinite extent, T_∞–T_b constant
(iv) constant liquid temperature T_∞ in the whole domain except in a thin "thermal boundary layer" surrounding the bubble, where T_∞ drops to T_b, see Fig. 10(a)
(v) heat transfer from liquid to vapour through heat conduction in the "thin thermal boundary layer"
(vi) inviscid Newtonian liquids
(vii) during the growth, purely radial and laminar liquid motion

Plesset and Zwick [79] demonstrated that the Rayleigh equation, without considering the cooling effect caused by evaporation, over-predicts the growth rate of steam bubbles in water significantly at around 100 °C. A plot of the bubble radius as a function of the time is shown in Fig. 10(b) for a temperature of 103.05 °C.

Nevertheless, the validity range of the Plesset and Zwick correlation is largely limited due to the numerous simplifications made

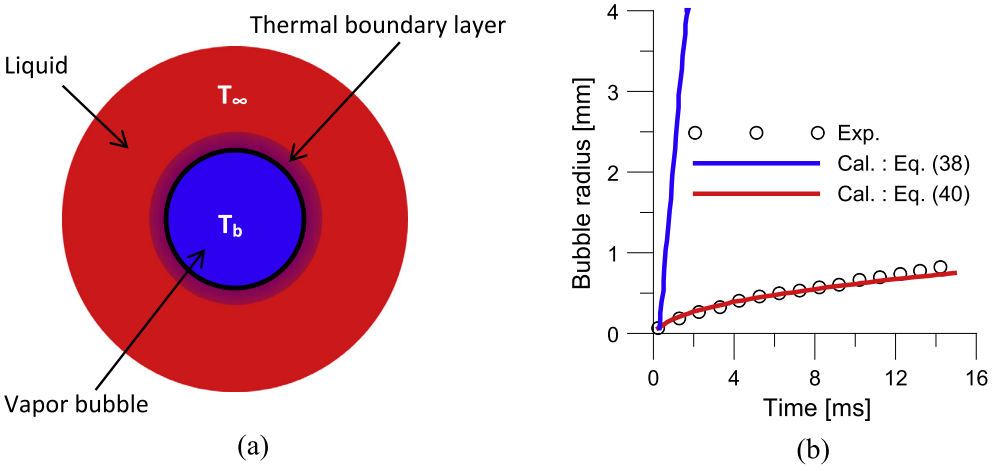

Fig. 10. (a) "Thermal boundary layer" assumption in the derivation of Plesset and Zwick [79] correlation; (b) Comparison with the experimental data of Dergarabedian and Pasadena [83] for 1 atm water and the prediction with the Rayleigh equation.

in its derivation. As pointed out by Avdeev [82] "...the Plesset-Zwick formula, which is commonly accepted in computational practice, is not applicable at both small and large Jakob numbers ..."

Based on Eqs. (38) and (40) some general relations were derived, which are applicable to both inertia-controlled and thermally-controlled bubble growth, e.g. [84,85]. However, in practical cases the assumptions assisting the derivation of Eq. (40) are usually not met. In addition, the asymptotic solution given in Eq. (40) could result in serve underestimation of the heat transfer rate in cases where convection prevails. According to Wallis [86], in most cases the convective contribution to heat transfer is dominant in comparison with transient conduction. Aleksandrov et al. [87] suggested that the effect of translational motion on bubble growth can be accounted for by a factor

$$\left(\frac{dR_b}{dt}\right)_{V_{lg}\neq 0} = \left(\frac{dR_b}{dt}\right)_{V_{lg}=0}\left(1+\frac{2}{3}\frac{V_{lg}t}{R_b}\right)^{1/2}. \tag{41}$$

Here the translational velocity V_{lg} is constant in direction and quantity. Nevertheless, in real situations, the relative motion between vapour bubbles and surrounding liquid is irregular and multi-dimensional. Therefore, in most investigations the interphase mass and heat transfer problem is solved numerically instead of analytically.

To evaluate the weight of inertial and thermal effects on the cavitation bubble growth, Kato [88] adopted the Jakob number and a non-dimensional time, t^*,

$$t^* = \frac{t}{a_l \frac{\rho_l}{P_{sat}(T_\infty)-P_\infty(t)}}. \tag{41a}$$

They suggested that the thermal effect is large at large t^* and low Jakob number.

The non-dimensional temperature drop, termed the B-factor, has often been used for the characterization of thermal effect on cavitation dynamics [89].

$$B = \frac{T_\infty - T_{sat}}{\rho_g L/\rho_l C_P}. \tag{42}$$

Alternatively, Brennen [90] scales the thermodynamic effect by introducing a purely thermo-physical quantity ξ. He suggested that the relative magnitude of the inertial and thermal terms changes with the time. At the beginning bubble growth is purely inertial-controlled while thermal effects become significant after a critical time point t_{cr},

$$t_{cr} = \frac{P_{sat}(T_\infty)-P_\infty(t)}{\rho_l}\cdot\frac{1}{\xi^2}. \tag{43}$$

This implies that the thermal effect is dominant at high temperature, since ξ increases with the liquid temperature. For example, under a tension of 10^4 kg/m s^2, the critical time for water at 20 °C is of the order of 10 s while for water at 100 °C is about 10 μs, which is near the lower limit of experimental observation.

It is worth noting that the applicability of all above parameters is severely restricted due to simplifications and assumptions involved in their derivation. As a result, in a given case judging whether the inertial or thermal effect is negligible or not remains still an open topic.

The impact of thermodynamic effect on the cavitation dynamics has received much attention [85,91–96]. One usual way is to perform modifications based on the traditional cavitation model or the simplified Rayleigh-Plesset equation. For example, Zhang et al. [85] extended Eq. (38) by superposing a thermal term linearly:

$$\frac{dR_b}{dt} = \underbrace{\sqrt{\frac{2}{3}\frac{P_{sat}(T_\infty)-P_\infty(t)}{\rho_l}}}_{\text{inertial}} + \underbrace{\sqrt{\frac{3}{\pi}}\frac{\rho_l C_P(T_\infty - T_{sat})}{\rho_g L}\sqrt{\frac{a_l}{t}}}_{\text{thermal}}. \tag{44}$$

In contrast, the impact of the inertial effect under flashing conditions has received little attention. In commercial CFD software, it is often assumed that the pressure field is shared by all fluids, see Fig. 11(c). In this situation, it is difficult to take into account the effect of pressure difference at the interface on bubble growth and vapour generation unless additional momentum source terms are added.

2.4. Vapour generation rate

Numerical studies of flashing flows are directed towards the determination of vapour generation rate, for which three ways have been employed in the literature. One of them treats the transition of the thermodynamic system from non-equilibrium to equilibrium as a relaxation process. The two states are bridged by means of an empirical coefficient, i.e. the relaxation time. This approach is termed the Homogeneous Relaxation Model (HRM). The others are based on the observations of either bubble dynamics or interfacial exchange.

2.4.1. HRM model

The HRM model was first applied to flashing cases by Bilicki and Kestin [97] and has subsequently been frequently adopted, e.g. in Neroorkar et al. [10], Faucher et al. [98], Angielczyk et al. [99], Gopalakrishna and Schmidt [100], Neroorkar [101] and Ramcke and Pfitzner [102]. According to this model, the volumetric vapour generation rate can be expressed as:

$$\Gamma_g = \left.\frac{\partial\rho}{\partial x}\right|_{P,h}\cdot\frac{dx}{dt} = \left.\frac{\partial\rho}{\partial x}\right|_{P,h}\cdot\left(\frac{\bar{x}-x}{\Theta}\right), \tag{45}$$

where ρ is the density of the liquid-vapour mixture, and x is vapour quality referring to mass fraction of vapour. The partial differential $\left.\frac{\partial\rho}{\partial x}\right|_{P,h}$ is caused by non-equilibrium effects of the system. The equilibrium quality $\bar{x}$ (P, h) is usually obtained from a look-up table. The instantaneous quality and void fraction is related to the density, which is obtained from the solution of the continuity equation, as follows:

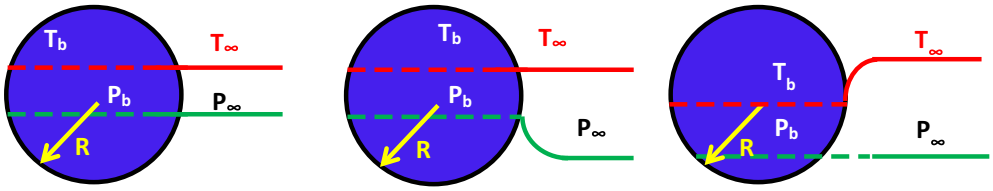

(a) Mechanical & thermal equilibrium (b) Thermal equilibrium (c) Mechanical equilibrium

Fig. 11. Assumption of mechanical or thermal equilibrium between bubble and surrounding liquid in the modelling.

$$x = \frac{\alpha\rho_g}{\rho}, \alpha = \frac{\rho_l - \rho}{\rho_l - \rho_g}.$$

The most important consideration in using the HRM model is the formulation of the relaxation time. A well-accepted empirical relation was presented in Downar-Zapolski et al. [103]:

$$\Theta = \Theta_0 \alpha^a \psi^b. \quad (46)$$

For lower pressures, e.g. $P \leq 10$ bar, the recommended coefficients are:

$\Theta_0 = 6.51 \times 10^{-4} s$,
$a = -0.257$,
$b = -2.24$, and
$\psi = \frac{P_{sat}-P}{P_{sat}}$

For higher pressures, the values are:

$\Theta_0 = 3.84 \times 10^{-7} s$,
$a = -0.54$,
$b = -1.76$, and
$\psi = \frac{P_{sat}-P}{P_{cr}-P_{sat}}$,

where P_{cr} is the critical pressure.

2.4.2. Bubble growth model

An alternative method for the estimation of vapour generation rate is from point view of bubble dynamics and bubble growth.

$$\Gamma_g = \rho_g N_b \cdot \frac{dV_b}{dt} = \rho_g A_i \frac{dR_b}{dt}. \quad (47)$$

The prerequisite of such an approach is that a reliable analytical expression for the growth rate dR_b/dt is available. Some typical correlations are presented above in Section 2.3 bubble growth. Nevertheless, bubble growth in practical superheated flows for example with three-dimensional velocity and pressure gradients is often sufficiently complex to prevent any analytical solution.

2.4.3. Interfacial exchange model

The more popular and general approach is to postulate that phase change is induced by interphase heat transfer. The vapour generation rate during evaporation is related to heat flux via

$$\Gamma_g = A_i \frac{\dot{q}}{L}, \quad (48)$$

where $\dot{q}$ is the total heat flux transferring from both vapour and liquid to the phase interface, and A_i is the interfacial area density.

For vapour-liquid such as steam-water mixtures under most practical conditions, the interfacial heat transfer on the vapour side is usually much smaller (less than 5%) than in the liquid phase [104]. Therefore, it is usually ignored by assuming that the temperature is uniform inside the bubble and equal to that at the interface, and

$$\dot{q} = \dot{q}_{l\to \mathrm{int}} = h_{tc}^{l}(T_l - T_{sat}), \quad (49)$$

where h_{tc}^{l} is the overall heat transfer coefficient between surrounding liquid and the interface, which is always at the saturation condition.

Therefore, the primary concern in evaluation of vapour generation rate using the two-fluid model is to estimate appropriately the heat transfer coefficient on the liquid side. There have been a variety of analytical and empirical correlations published in open literature such as [87,105–107]. They take into account either the effect of conduction or translational convection, or both of them. Almost all of them are limited to isolated small spherical bubbles, which can be treated as solid interfaces. The effect of deformation, rotation and interference of bubbles as well as turbulence is often ignored. Although few correlations were presented, e.g. by Dobran [22] and Schwellnus and Shoukri [108], for the annular flow regime, the mechanism of heat transfer between large irregular gaseous structure and surrounding liquid remains still an open topic for investigation. A detailed review on the limitation of existing models was carried out in our previous work [109].

In a word, the applicability of the sophisticated method is restrained largely by the reliability of closure models representing interactions between the phases.

2.5. Interfacial area density

The uncertainty involved in the determination of interfacial area density A_i affects the prediction of vapour generation rate as well as other interfacial exchanges significantly. It is known that in a gas-liquid flow, not only the size and number density but also the shape of bubbles change as a function of gas volume fraction, flow parameters, interface and fluid properties. Consequently, the morphology of gas-liquid interface and the flow regime vary continuously. In different flow regimes A_i should be computed in different ways.

The difficulty is that up to now there is no efficient method to capture the dynamic transition between flow regimes. Moreover, available models are limited to certain flow regimes, where the interfacial morphology is well defined, e.g. bubbly flow (or droplet flow) and annular flow (or stratified flow). Little is known about intermediate flow regimes such as churn-turbulent flow, bubbly-slug flow, and annular-mist flow.

In vast majority of theoretical work on bubbly flow or droplet flow, the interfacial area density is computed with the assumption of spherical shape and constant size, i.e.

$$A_i = 4\pi R^2 N_b = \frac{6\alpha}{d_b}. \quad (50)$$

In Dobran [22], Richter [23], and Schwellnus and Shoukri [108], the interfacial area density in churn-turbulent flow ($\alpha_B < \alpha < \alpha_A$) is computed by means of a linear interpolation between the bubbly and annular regimes:

$$A_i = A_{i,B} + \frac{A_{i,A} - A_{i,B}}{\alpha_A - \alpha_B}(\alpha - \alpha_B), \quad (51)$$

where $\alpha_B = 0.3$ and $\alpha_A = 0.8$ is the gas volume fraction at the upper limit of bubbly flow and the start of annular flow, respectively.

$$A_{i,B} = \frac{6}{d_b}\alpha_B, \quad (52)$$

and

$$A_{i,A} = \frac{4}{D_p}\alpha_A^{1/2}, \quad (53)$$

where D_p is the inner diameter of the pipe.

Wu et al. [29], Saha et al. [110] and Blinkov et al. [75] observed that in their cases bubbly-slug flow prevails in the range of $\alpha = 0.3$–0.8. They estimated the interfacial area density for such flow regime as a sum of small spherical bubbles and Taylor bubbles, i.e.

$$A_i = \frac{6(\alpha - \alpha_T)}{d_b} + \frac{4\alpha_T^{2/3}}{\alpha_{s,\max}^{1/6} D_p}, \quad (54)$$

where α_T is the volume fraction of Taylor bubbles.

In addition, the effect of nucleation, coalescence and breakup can be taken into account by introducing an additional transport equation for the total bubble number density or interfacial area concentration directly. More details can be found in the work of Kolev [69], Maksic and Mewes [76], Chang and Lee [111], Hibiki

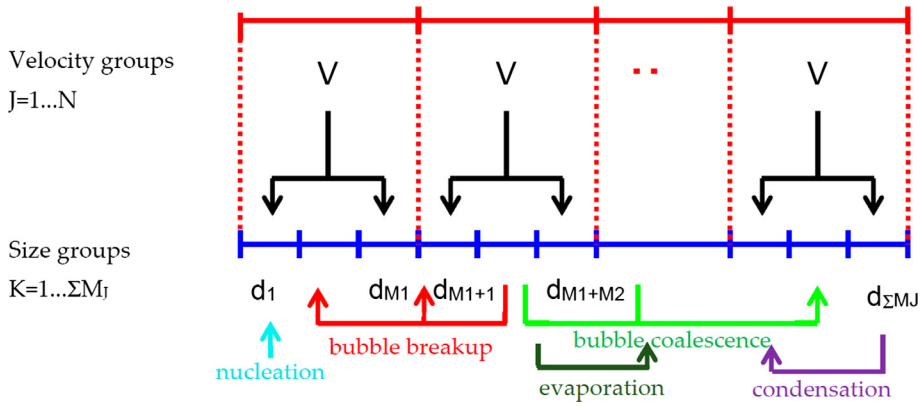

Fig. 12. Schema of the inhomogeneous MUSIG model [114].

and Ishii [112] and Marsh and O'Mahony [113]. Nevertheless, as pointed out by Laurien [25], formulations able to take into account the spectrum of local bubble sizes, namely poly-disperse approaches (such as MUSIG: the Multiple Size Group model), are more close to the reality than the mono-disperse ones.

The schema of the inhomogeneous MUSIG model is shown in Fig. 12, where the gaseous phase consists of N velocity groups and M ($=\Sigma M_J$) size groups. In other words, N momentum equations and M size fraction equations considering various sub-phenomena such as coalescence and breakup are solved. Finally, local mean bubble size is obtained from the size fractions.

Recently, a general relation was proposed by Hänsch [115]. It is an extension of the original MUSIG model [114] and expected to be applicable for the whole flow regime from dispersed bubbles to continuous gaseous structures. It blends the interfacial area density for the poly-disperse and the continuous morphology in following way

$$A_i = (1 - \varphi_{morph})A_{i,bubb} + \varphi_{morph}A_{i,cont}, \tag{55}$$

where φ_{morph} is a blending function. The interfacial area density for large gas structure, $A_{i,cont}$, is determined from free surface and dispersed droplet flow, i.e.

$$A_{i,cont} = \max(A_{i,fs}, A_{i,drop}), \tag{56}$$

where $A_{i,fs}$, $A_{i,drop}$ are the interfacial area density of free surface and dispersed droplet flow, respectively.

3. Modelling of flashing flows

Since the middle of last century, a significant amount of literature has been published on the modelling of two phase mixtures generated by the flashing process. Most studies focus on the critical flow problem because of its relevance to the safety of pressurized water nuclear power plants. In general, the single-phase Bernoulli equation overestimated the actual critical flow rates, while the homogeneous equilibrium ones underestimated them [34]. The vast amount of literature can be classified according to various criteria. The current work is focused on two of them, i.e. the treatment of interphase non-equilibrium and the level of spatial resolution (component-oriented or CFD).

There are three essential factors that have to be considered in the modelling of flashing phenomena [7]:

(1) Spatial and temporal dependence of pressure. It is necessary for the evaluation of the fluid thermodynamic properties.
(2) Relative velocity between the phases. It is of great importance for a reliable prediction of interphase mass and heat transfer.
(3) Thermal non-equilibrium between liquid and vapour phases.

Generally, the quantities of interest in the modelling of two-phase flows are:

(1) Void fraction α;
(2) Vapour quality x;
(3) Pressure P_l, P_g;
(4) Velocities u_g, u;
(5) Internal energy (or enthalpy) H_g, H_l.

The quality x can be determined on the basis of the void fraction or vice versa, once the pressure and the ratio between the velocities of the two phases are known. Thus the problem reduces to a total of seven unknowns.

Various methods have been employed to model the two-phase flow with different levels of complexity. Depending on the degree of simplification, non-equilibrium effects are either ignored completely or considered partially or fully, and the number of solved equations increases from 3 to 7 correspondingly. Typical models with representative literature are summarized in Fig. 13 below. Most methods have been implemented in one-dimensional system codes. Recently, more and more investigations using two or three-dimensional Computational Fluid Dynamics (CFD) have been published, which are highlighted by red colour in Fig. 13. In comparison to the component-oriented approach, the CFD technology has the advantage of providing detailed information about the spatial distribution of the phases. The state of art of CFD modelling of flashing flows is given in a separate section below.

The classification of the models is first based on whether thermal non-equilibrium is considered or not, and then whether the fluid dynamic behaviour in terms of interfacial relative motion is considered or not, i.e. with or without slip. As mentioned above, most of the investigations are based on pressure equilibrium and the mass transfer rate is evaluated by interphase heat transfer [116–149]. Nevertheless, there are some exceptions such as Xing and Frankel [150], Palau-Salvador et al. [151], and Ishigaki et al. [152]. These investigators applied cavitation models to flashing phase change (or thermal cavitation), where the mass transfer rate is evaluated by the bubble radius and the pressure drop across the interface. Liu et al. [96] proposed a thermodynamic cavitation model, which is applicable to high temperature conditions. In addition, the application of two-pressure two-fluid model to flashing flows has been discussed by some authors such as Ruan [35] and Banerjee [104]. It assumes that the pressure inside each phase is uniform up to the interface, where a pressure discontinuity is allowed. The model consists of seven balance equations of volume,

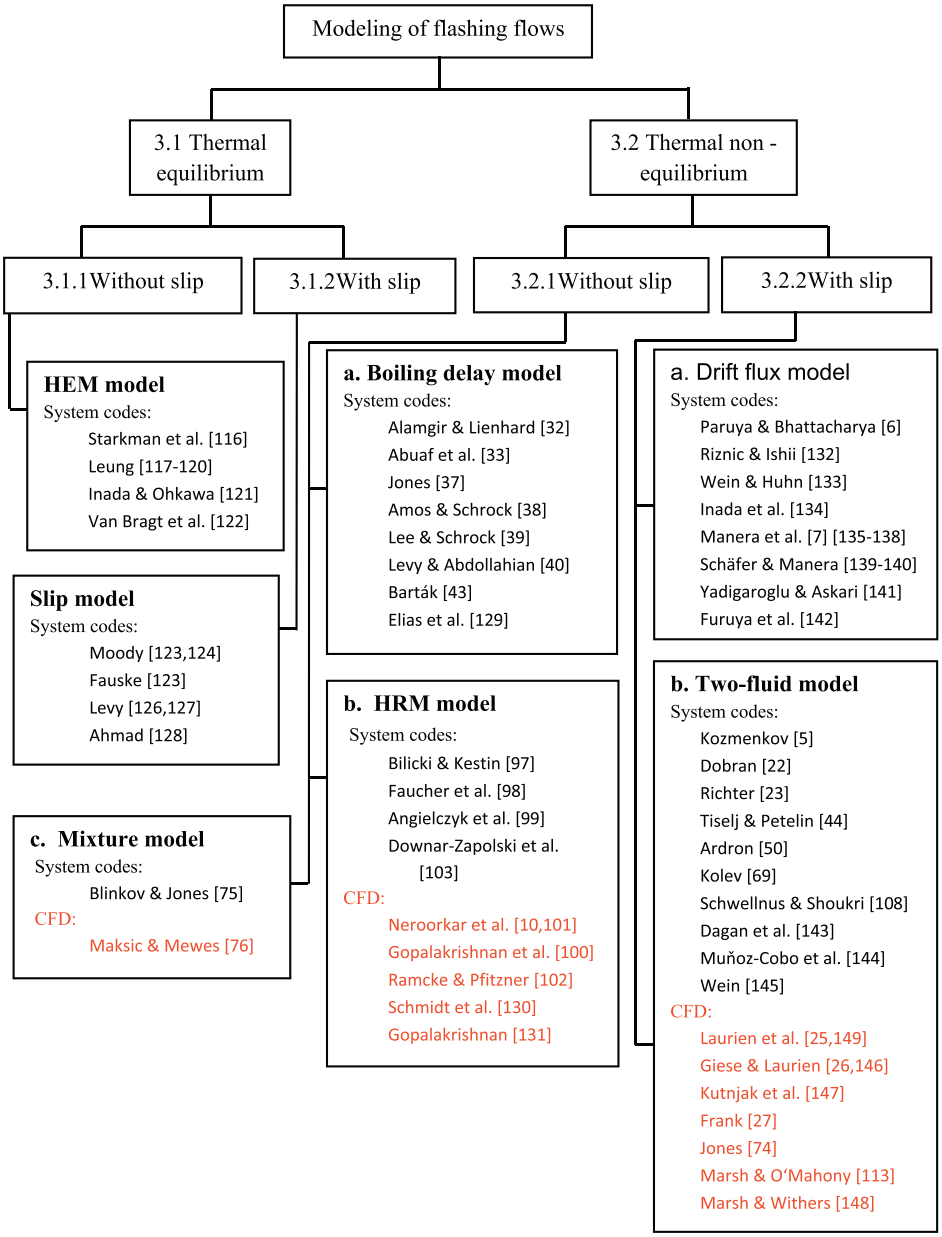

Fig. 13. Classification of models for modelling of flashing flows.

mass, momentum and energy. In Fig. 13 only pressure equilibrium models are summarized.

3.1. Thermal equilibrium

Models belonging to this category are characterized by the following local equilibrium conditions:

$$T_g = T_l. \tag{57}$$

This implies that the heat transfer rates are infinite at the interface so that the two phases are always in thermal equilibrium. Depending on whether the interphase slip velocity is considered or not, the model can be classified further into two branches, i.e. without slip and with slip.

3.1.1. Without slip

If no slip between the liquid and the vapour phases is considered, there is:

$$\vec{U}_g = \vec{U}_l. \tag{58}$$

With the conditions in Eqs. (57) and (58) the two-phase mixture behaviours like a pseudo single-phase fluid. All thermodynamic properties such as density, internal energy, viscosity, and thermal conductivity are obtained from interpolation tables or "equation of state", and weighted by the equilibrium quality x_e in the usual manner as

$$y = y_l + x_e(y_g - y_l), \tag{59}$$

where y represents a property and the subscripts l, g indicate liquid and vapour phase, respectively.

This type of model is called a Homogeneous Equilibrium Model (HEM), i.e. a 3-equation model. Due to its simplicity and high computational efficiency the isentropic HEM model is the basis of early versions of several system codes such as RELAP. It has been used very often in the modelling of flashing phenomena in critical flow, e.g. in Starkman et al. [116], Leung [117–120], Inada and Ohkawa [121] and Van Bragt et al. [122]. However, its restriction is inherent and notorious, which was evaluated in Wallis [86] and Yang et al. [153]. In principle, it is inappropriate for short flow channels,

where the time is insufficient for the two-phase mixture to proceed to equilibrium, and for cases with large difference in phase velocities, e.g. annular flow. For example, the underestimation of critical flow rates for short pipes can reach a factor of 1/5. Therefore, more and more investigations focus on methods incorporating the non-equilibrium effects. They range from empirical to physically-based models.

3.1.2. With slip

According to Richter [23] as bubbles grow and void fraction exceeds a value of about 0.3, relative motion between the phases becomes important and ignoring it will introduce significant errors. The simplest method accounting for the interphase velocity difference is to introduce an analytical or empirical correlation for the slip ratio, S, which is termed **slip model** in Fig. 13. Based on the assumption of energy balance and an isentropic process Moody [123,124] derived following expression for S:

$$S = \left(\frac{\rho_l}{\rho_g}\right)^{1/3}. \tag{60}$$

For non-isentropic flow, Fauske [125] obtained the following slip ratio assuming momentum is balanced.

$$S = \left(\frac{\rho_l}{\rho_g}\right)^{1/2}. \tag{61}$$

Practice shows that the Fauske or Moody models compensate for the underestimation of critical flow rate by the HEM model using unnaturally high values of slip ratios [34]. A further improvement was proposed by introducing an empirical pre-factor, which lies between 0.5 and 1.0.

In addition, numerous correlations, which are not restricted to critical flow conditions, are available for the estimation of local slip ratios such as Levy [126,127] and Ahmad [128].

3.2. Thermal non-equilibrium

Various experimental studies reveal that the critical flow rate increases rapidly as the pipe length reduces. For short pipes the actual flow rates are much larger than the predictions of above models. The discrepancy has to be attributed to thermal non-equilibrium effects [34].

The thermal non-equilibrium between the gaseous and liquid phases is expressed as:

$$T_g \neq T_l. \tag{62}$$

As mentioned previously, it is often assumed that the vapour phase always stays at the saturation temperature corresponding to the bulk pressure, i.e. $T_g = T_{sat}$. If superheated vapour is allowed, an appropriate relation for the heat transfer coefficient between the vapour and the interface is necessary to ensure the vapour temperature remaining slightly above the saturation one [77]. Otherwise, the simulation can lead to unphysical results with subcooled vapour.

3.2.1. Without slip

Numerous investigations aimed to capture the thermal non-equilibrium effect but not velocity difference in the vaporization process. Henry et al. [154,155] attempted to describe the thermal non-equilibrium effect on critical flow rate by introducing a characteristic parameter of the system, which was calculated from their experimental studies. Other theoretical models shown below can be classified into three sub-categories, namely, boiling delayed model, HRM model and mixture model.

3.2.1.1. Boiling delayed model. The idea of this type of model has been already discussed in Sections 2.1 and 2.2.2 above, e.g. [32,33,37–40]. It suggests that the bubble nucleation begins at a certain degree of superheat in the liquid. The delay in nucleation limits the vapour generation rate thereafter. The "pressure-under shoot", i.e. the difference between the flashing inception pressure and the saturation one, is determined by simplifying assumptions or semi-empirical relations. For example, Lackmé [156] assumed that flashing inception pressure is about 95% of the saturation pressure. This assumption is however only reasonable within a narrow range of pressure. More recently, Alamgir and Lienhard [32] and Barták [43] and Elias and Chambré [45,129] investigated the boiling-delayed phenomenon in more detail both experimentally and theoretically. Several models have been proposed, e.g. Eqs. (3)(10).

In their 1D steady-state simulation, Lee and Schrock [39] first determined the flashing inception position using the pressure-undershoot relation. In the region prior to this position the standard single-phase equation was used. Beyond flashing inception, two-phase mixture conservation equations without interphase slip or any transfer terms are considered. The vapour phase was assumed to be saturated at the local pressure, while the liquid phase is assumed to be superheated. Properties of the metastable liquid were evaluated by extrapolation of the equation of state for subcooled region. As discussed in Section 2.1, reliable equations of state for metastable liquid are still missing. Heat transfer from liquid to the two-phase interface is accounted for by a liquid superheat relation.

3.2.1.2. HRM model. As stated above in the last section, the HRM model attempts to correct the HEM model by introducing an empirical thermal relaxation time Θ. It implies that the two-phase mixture is in thermal non-equilibrium, which relaxes to its final equilibrium status over the period of Θ. As a result, the actual void fraction or vapour generation rate is smaller than that predicted by the HEM model. More details and application examples are given in Section 2.4.1 and Fig. 13. CFD examples are [100–102,130,131].

3.2.1.3. Mixture model. Another representative model assuming mechanical equilibrium is the mixture model. In their one-dimensional, transient simulation of flashing flow in nozzles Blinkov [75] solved two continuity equations for the mixture and the vapour phase, one momentum equation for the mixture, one energy equation for the liquid while vapour temperature assumed to be at local saturation conditions, and one bubble transport equation to describe the nucleation effect. Constitutive equations are required for the determination of vapour generation rate, friction force and nucleation rate. The vapour generation rate is computed according to Eq. (48). Heat input from the liquid to the bubble-liquid interface as well as the interfacial area density is treated in different ways for different flow regimes. A similar **4-equation** model was adopted in [76] for CFD calculation of flashing flows in pipes and nozzles. They applied the Jones nucleation model and the Labuntzov [105] heat diffusion model for interphase mass and heat transfer.

3.2.2. With slip

Liao [109] showed that the velocity slip is of great importance for a reliable prediction of flashing flows. Neglect of it may lead to significant underestimation of vapour generation rate. In principle, two momentum equations should be solved for liquid and vapour velocities separately. Nevertheless, drift-flux models can be used to approximate the phase slip by means of other variables such as void fraction and densities. They have been widely used in thermal-hydraulic codes for nuclear safety analysis, e.g. [132–142].

3.2.2.1. Drift-flux model. According to one-dimensional drift-flux model, vapour velocity is given by:

$$u_b = C_0 J + \langle\langle V_{gj} \rangle\rangle. \tag{63}$$

Here C_0 is the distribution parameter accounting for the slip due to phase and velocity distributions and $\langle\langle V_{gj} \rangle\rangle$ is the averaged local drift velocity for the local slip between phases. Both of them have to be provided by some closure correlations. For example, in Riznic and Ishii [132] and Furuya et al. [142] the drift flux formulation proposed by Ishii [157] was used, whereas Paruya and Bhattacharya [6] applied the oldest Zuber and Findlay [158] model. These semi-empirical relations are mostly based on experience gained in air-water flow while little is known about steam-water flows with phase change. The suitability of drift-flux models for flashing flow inside a vertical pipe was tested by Manera [7]. Representative models for nuclear applications were selected from the literature. The GE-Ramp model [159] was found to work very well.

Although in principle it is possible to consider the slip between phases using a drift-flux model in frame of the HEM model, the majority of examples listed in Fig. 13 are an extension of the above 4-equation mixture model. This is because a model with separate temperature fields for two phases is more reliable than the HEM model with some subcooled boiling models for thermal non-equilibrium effects [7]. On the other hand, it is a good compromise in terms of reliability and complexity.

A **5-equation** drift-flux model was presented in Paruya and Bhattacharya [6]. They solved mass-conservation equations for the liquid and vapour, momentum equation for two-phase mixture, the energy-conservation equations for the mixture and liquid. That means that the assumption that vapour is always saturated is discarded. A slightly different model was used by Schäfer and Manera [139,140] and Manera [136–138], in which the liquid continuity equation of the liquid is replaced by that of the mixture, and the energy equation of the mixture replaced by that of the vapour.

3.2.2.2. Two-fluid model. Till now the most general and sophisticated model for the description of flashing phenomenon is the **6-equation** model, i.e. the two-fluid model (TFM). It consists of two mass balance equations of liquid and gas phases, two momentum equations and two energy equations. All the interaction and non-equilibrium exchanges between the two fluids are modelled by additional constitutive relations. In the practice it is often reduced to a 5- or 4-equation model by applying some simplifying assumptions. For example, the energy equation for the vapour phase becomes superfluous if saturated vapour assumed.

In contrast to the preceding models, one attractive feature of the TFM is that it has the potential to capture not only the thermal non-equilibrium effects but also the slip between the fluids in a way much more accurate than the drift-flux model. There is a consensus that improvements are possible by developing a set of separated conservation equations for each phase and using phase interaction models to describe the flow behaviour during flashing [160–162]. The application of TFM formulation has proved to be quite promising since a large variety of flow regimes can be modelled using the same set of equations provided appropriate closure models are available [143–145]. However, one cannot expect the TFM to overcome all empiricism in such a complex flow situation where heat, mass and momentum transfer are present simultaneously [23]. The accuracy of TFM in the prediction of flashing problem is limited by closure models. The more the amount of physics that one chooses to incorporate in the model, the more the constitutive models are required. To answer the question where the limitations of the TFM for flashing flows are hidden it is helpful to evaluate the closure models characterizing all interphase exchanging processes.

3.3. CFD simulation of flashing flows

As mentioned at the beginning, so far system codes have been routinely applied for the simulation of flashing flows. Nevertheless, the flow is often embossed with three-dimensional natures, namely, large heterogeneous gaseous structure and high gas volume fraction. Ever-increasing computational power facilitates the use of highly-resolved CFD techniques to simulate multiphase flow phenomena. Recently, promising CFD research on flashing flows have been published such as in Laurien [25], Giese and Laurien [26,146,149], Kutnajk et al. [147], Frank [27], Marsh and O'Mahony [58], Maksic and Mewes [76], Marsh and Withers [148], Mimouni et al. [77] and Janet et al. [78]. All these simulations are based on the framework of a simplified two-fluid-model.

In contrast to system codes, where various flow regimes can be considered with the help of steady-state flow regime maps, CFD modelling of flow regime transition is still in the way of development. In all published work on flashing flows the vapour phase is treated as discrete spherical bubbles. Local volumetric void fraction α is related to bubble size d_b and number density N_b by:

$$\alpha = \frac{\pi}{6} d_b^3 \cdot N_b, \tag{64}$$

Two of the three parameters have to be determined. The void fraction α is provided by the continuity equation. Additional assumptions or transport equations for d_b or N_b are required to complete the equation. Based on this criterion, the numerical method can be divided into mono-disperse and poly-disperse. So far, most published work on modelling of flashing flows falls into the former category. They prescribe a constant bubble size (or number density) or solve the bubble transport equation additionally. That means that the bubble size in each computational cell has a single value instead of a spectrum at any given time. Whereas some general agreement exists on the modelling framework (i.e. mono-disperse Two-Fluid), for the interfacial area and interphase exchange different closure models must be applied, e.g. for nucleation and interphase heat transfer.

Laurien and his co-workers had studied the flashing phenomenon experimentally and theoretically in 2001. They simulated water evaporation and re-condensation phenomena caused by steady-state pressure variation inside a three-dimensional complex pipeline [25,26,146,149]. Frank [27] simulated the well-known Edwards pipe blow-down test [4], which is the international standard problem No. 1 sponsored by the NEA Committee on the Safety of Nuclear Installations, using a one-dimensional simplified mesh in ANSYS CFX. Both of them employed a 5-Equation model including two continuity equations, two momentum equations for liquid and vapour, respectively, and one energy equation for liquid. The vapour was assumed to remain always at the saturation condition corresponding to local pressure, which is uniform inside and outside the bubble. The assumption is reasonable in case of small depressurization rate. For the computation of interfacial area density a constant bubble diameter, e.g. d_b = 1 mm, is prescribed in the whole domain. In addition, the momentum interaction between the gas and liquid phases is modelled only as a drag force. A similar model with both drag and non-drag forces was presented in Liao et al. [28], where the flashing of water inside a large vertical pipe due to the opening of a blow-off valve was simulated.

Later on, Laurien [25] suggested that a model presuming bubble number density instead of bubble size, which allows bubble size to grow, and is more closely aligned to the physical picture of boiling flow. This assumption is acceptable when both the metastable zone and nucleation zone are sufficiently narrow (see Fig. 4), and bubble dynamics such as coalescence and break-up are negligible. Otherwise, an additional transport equation for the bubble number

density with appropriate source terms, or even a poly-disperse method is necessary. Meanwhile, Pinhasi et al. [8] found that models based on this assumption tend to under-predict the vapour generation rate.

Maksic and Mewes [76] simulated flashing flows in pipes and nozzles by using a 4-Equation model, where a common velocity field is assumed for both phases. The inter-phase heat transfer is assumed to be dominated by conduction. However, it has been shown that in most flashing expansion cases the convective contribution due to relative motion of bubbles dominates the heat transfer [84]. Neglecting of inter-phase velocity slip obviously under-predicts vapour generation rate [109]. Wall nucleation was considered as a unique source of bubble number density in the additional transport equation. The Jones model [70] [75,164,165] was used to determine the nucleation rate. Inter-phase mass, momentum and energy transfer due to nucleation was ignored.

Marsh and O'Mahony [58] simulated the nozzle flashing flow using a 6-Equation model in the commercial CFD code FLUENT, with separate mass, momentum and enthalpy balance equations for liquid and vapour. Inter-phase mass and momentum as well as energy transfer resulting from both nucleation and phase change were taken into account. However, the effect of non-drag forces on momentum exchange and the heat transfer between vapour and vapour-liquid interface were neglected. A modified version of Blander and Katz nucleation model [51] was employed for the computation of bubble nucleation rate. The original model was found to create large numerical instability, which is based on the classical homogeneous nucleation theory.

Mimouni et al. [77] simulated the cavitating flow using a 6-Equation model in NEPTUNE_CFD. The vapour temperature was ensured to be very close to the saturation temperature by using a special heat transfer coefficient. Besides the drag, added mass and lift force was included in the inter-phase momentum transfer. The contribution of nucleation to the vapour generation rate as well as momentum and energy transfer was considered by the slightly modified Jones model [70,75,163,164]. The original model was shown to be insufficiently general by the authors. Nevertheless, the effect of nucleation and vaporization on the mean bubble size was ignored, namely, a constant bubble size was assumed.

Janet et al. [78] studied the performance of various nucleation models in a flashing nozzle flow by using the 5-Equation model in CFX version 14.5. It was found that predictions obtained with the Jones model [75] are more reliable than the RPI [165] and Riznic models [132].

Recently, the perspective and limitation of current CFD technology for flashing flows was discussed by Liao and Lucas [166]. At the same time, poly-disperse attempts were made for flashing pipe flow under pressure release transients. Initially subcooled water circulates with a velocity of 1 m/s through a vertical pipe (DN200) under 10 bar. The depressurization and evaporation process is realized and controlled via a blow-off valve. The MUSIG approach introduced above (see Fig. 12) was used to predict the formation of vapour bubbles in superheated liquid and the change of bubble size due to phase change, coalescence and breakup. The Jones model [75] and Liao model [167] was employed to reproduce the nucleation and coalescence/breakup process, respectively. The comparison between calculated and measured bubble size distribution at four time points is shown in Fig. 14 below, where the horizontal axis is bubble size and the vertical one is the normalized void fraction of each size group. One can see that the evolution tendency is well captured by the MUSIG model. However, an obvious over-prediction of the bubble breakup rate especially at 59 s is

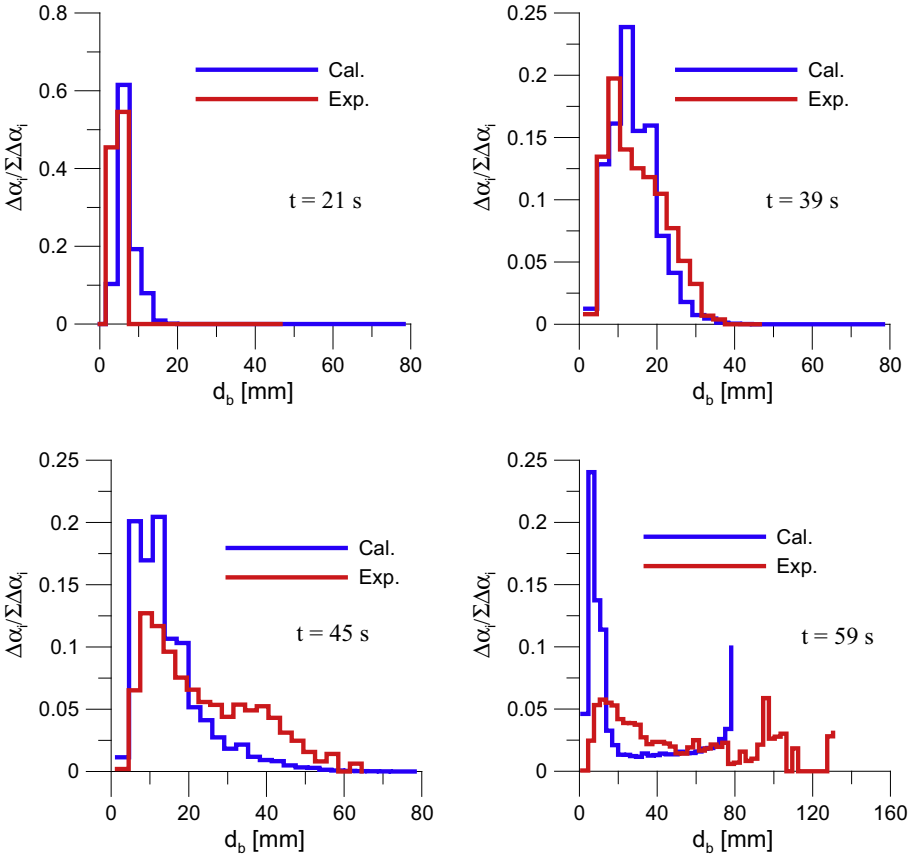

Fig. 14. Prediction of the evolution of bubble size spectrum during flashing with MUSIG.

observed. On the other hand side, the broad size spectrum evidences that a poly-disperse model instead of the mono-disperse one is necessary in this case.

4. Conclusion

The current review reveals the important physics and mechanisms that dominate the flashing process. An overview of the state of the art for theoretical models on these mechanisms is presented. Special attention was paid to the review of models for flashing inception, nucleation, bubble growth, vapour generation as well as interfacial area density. The current state of the art can be summarized as follows:

- The phenomenon of superheating is well-known in a boiling process, whereas the attainable superheat limit in a practical system is hardly predictable. Nucleation inception is strongly affected by liquid properties, impurities, wall surface characteristics as well as initial temperature and decompression rate.
- Numerous methods and models have been presented to describe the metastable zone and nucleation inception. None has been found to be adequate, and practically all of them rely more or less on empiricism. In comparison to a "pressure-under shoot" correlation, models supplying the transient nucleation rate appear to have more generality. The most recent state of the art is to solve a transport equation for bubble number density, which can account for source (or sink) terms due to nucleation as well as other processes such as coalescence and breakup. Nevertheless, more promising is to include these terms in a poly-disperse approach for consideration of bubble size distributions, which has been widely used in adiabatic situations.
- It is generally accepted that both pressure and temperature non-equilibrium across the liquid-vapour interface play a role in bubble growing in superheated liquid. As yet, a quantitative mathematical description considering the two factors is limited to ideal conditions, e.g. inviscid and quiescent liquids, laminar and isothermal flow. In most modelling work, one of them is neglected but discussion about the uncertainty caused by the exclusion is scant. Thermal non-equilibrium has being deemed to be dominant in flashing of hot fluids.
- The most advanced method accounting for thermal-controlled vapour generation is to estimate it from the interphase heat flux. However, a generally applicable model for interphase heat transfer coefficient is still missing. For example, most existing correlations are restricted to certain mechanism, spherical bubbles and laminar flows. Consideration of turbulence, bubble shape and swarm effect is rare.
- Although in a few investigations using the system codes flow regime transition is considered, most work is limited to bubbly flow and the assumption of spherical shape.

For the general modelling of the flow, it is commonly recognized that two-fluid model is the most appropriate approach. All recent progress in CFD modelling was achieved within this framework. A full two-fluid model with two-velocity, two temperature and two-pressure fields is presented in Ruan [35]. Nevertheless, pressure non-equilibrium and discontinuity at the interface was ignored in almost all previous work. The predictive ability of the two-fluid model is largely limited by the closure models, e.g. for mean bubble size and interfacial exchange area. The need to further develop and improve models regarding all above aspects is clear. Meanwhile, more experimental data especially related to bubble size, liquid velocity and turbulence as well as phase distribution are needed to fully validate these models. Finally, it is shown that bubble size spectrum may be surprisingly broad (over 100 mm) in some flashing situations. The update of mono-disperse approaches to poly-disperse ones is necessary, which imposes however new challenges for modelling of size change such as bubble coalescence and breakup.

Acknowledgement

The authors would like to express great appreciation to Jon Paul Janet for his kind help in preparing the manuscript and constructive suggestions.

References

[1] E. Laurien, Kavitation, Volumensieden, Ausgasung – Vergleich neuer Modellierungsansätze, Technologietag des ERCOFTAC Pilot Center Germany South, Stuttgart, 30. September, 2005.
[2] R. Darby, On two-phase frozen and flashing flows in safety relief valves, J. Loss Prev. Process Ind. 17 (2004) 255–259.
[3] T. Lenzing, L. Friedel, J. Cremers, M. Alhusein, Prediction of the maximum full lift safety valve two-phase flow capacity, J. Loss Prev. Process Ind. 11 (5) (1998) 307–321.
[4] A.R. Edwards, T.P. O'Brien, Studies of phenomena connected with the depressurization of water reactors, J. Brit. Nucl. Energy Soc. 9 (1970) 125–135.
[5] Y. Kozmenkov, U. Rohde, A. Manera, Validation of the RELAP5 code for the modelling of flashing-induced instabilities under natural-circulation conditions using experimental data from the CIRCUS test facility, Nucl. Eng. Des. 243 (2012) 168–175.
[6] S. Paruya, P. Bhattacharya, Simulation of oscillations in boiling flow in a natural circulation evaporator, Chem. Eng. Commun. 196 (2009) 362–390.
[7] A. Manera, Experimental and Analytical Investigations on Flashing-Induced Instabilities in Natural Circulation Two-Phase Systems – Applications to the Startup of Boiling Water Reactors PhD Thesis, Delft University of Technology, Delft, 2003.
[8] G.A. Pinhasi, A. Ullmann, A. Dayan, Modeling of flashing two-phase flow, Rev. Chem. Eng. 21 (2005) 133–264.
[9] D. Kawano, H. Ishii, H. Suzuki, Y. Goto, M. Odaka, J. Senda, Numerical study on flash-boiling spray of multicomponent fuel, Heat Transfer—Asia, Research 35 (5) (2006) 369–385.
[10] K.D. Neroorkar, S. Gopalakrishnan, D.P. Schmidt, Simulation of flash-boiling in pressure swirl injectors, Proceedings of 11st Triennial International Annual Conference on Liquid Atomization and Spray Systems, Vail, Colorando, USA, 2009.
[11] R. Schmehl, J. Steelant, Computational analysis of the oxidizer preflow in an upper-stage rocket engine, J. Propul. Power 25 (2009) 771–782.
[12] G. Lamanna, H. Kamoun, B. Weigand, C. Manfletti, A. Rees, J. Sender, M. Oschwald, J. Steelant, Flashing behaviour of rocket engine propellants, Atomization Sprays 25 (2015) 837–856.
[13] B.S. Park, S.Y. Lee, An experimental investigation of the flash atomization mechanism, Atomization Sprays 4 (2) (1994) 159–179.
[14] B. Zuo, A.M. Gomes, C.J. Rutland, Modelling superheated fuel sprays and vaporization, Int. J. Engine Res. 1 (2000) 321–336.
[15] E. Sher, T. Bar-Kohany, A. Rashkovan, Flashing-boiling atomization, Prog. Energy Combust. Sci. 34 (2008) 417–439.
[16] T. Bar-Kohany, M. Levy, State of the art review of flashi-boiling atomization, Atomization Sprays 26 (12) (2016) 1259–1305.
[17] R.C. Reid, Superheated liquids, Am. Sci. 64 (1976) 146–156.
[18] J.H. Lienhard, Md. Alamgir, M. Trela, Early response of hot water to sudden release from high pressure, ASME J. Heat Transf. 100 (1978) 473–479.
[19] C.T. Avedisian, The homogeneous nucleation limits of liquids, J. Phys. Chem. Ref. Data 14 (1985) 695–729.
[20] J.H. Lienhard, A. Karimi, Homogeneous nucleation and the spinodal line, ASME J. Heat Transf. 103 (1981) 61–64.
[21] K. Wolfert, Die Berücksichtigung thermodynamischer Nichtgleichgewichtszustände bei der Simulation von Druckabsenkungsvorgängen PhD Thesis, Technical University of Munich, Munich, 1979.
[22] F. Dobran, Nonequilibrium modelling of two-phase critical flows in tubes, ASME J. Heat Transf. 109 (1987) 731–738.
[23] H.J. Richter, Separated two-phase flow model: application to critical two-phase flow, Int. J. Multiph. Flow 9 (1983) 511–530.
[24] E. Valero, E. Parra, Reactor pressure analysis at the initial stage of a loss of coolant accident, Ann. Nucl. Energy 30 (2003) 585–601.
[25] E. Laurien, Influence of the model bubble diameter on three-dimensional numerical simulations of thermal cavitation in pipe elbows, Proceedings of 3rd International Symposium on Two-Phase Flow Modelling and Experimentation, Pisa, 22–24 September 2004.
[26] T. Giese, E. Laurien, Experimental and numerical investigation of gravity-driven pipe flow with cavitation, Proceedings of 10th International Conference on Nuclear Engineering (ICONE10), Arlington, Virginia, USA, April 14–18, 2002.

[27] Th. Frank, Simulation of flashing and steam condensation in subcooled liquid using ANSYS CFX, 5th Joint FZR & ANSYS Workshop: Multiphase Flows: Simulation, Experiment and Application, Dresden, Germany, April 26–27, 2007.
[28] Y. Liao, D. Lucas, E. Krepper, R. Rzehak, Flashing evaporation under different pressure levels, Nucl. Eng. Des. 265 (2013) 801–813.
[29] B.J.C. Wu, N. Abuaf, P. Saha, A study of nonequilibrium flashing of water in a converging-diverging nozzle Volume 2 - Modelling. U.S. Nuclear Regulatory Commission, Washington, D. C., 1981.
[30] M. Volmer, A. Weber, Keimbildung in übersättigten Gebilden, Zeitschrift für Phsikalische Chemie 119 (1926) 277–301.
[31] R. Becker, W. Döring, Kinetische Behandlung der Keimbildung in übersättigten Dämpfen, Ann. Phys. 24 (1935) 719–752.
[32] Md. Alamgir, J.H. Lienhard, Correlation of pressure undershoot during hot-water depressurization, ASME J. Heat Transf. 103 (1981) 52–55.
[33] N. Abuaf, O.C. Jones Jr., B.J.C. Wu, Critical flashing flows in nozzles with subcooled inlet conditions, ASME J. Heat Transf. 105 (1983) 379–383.
[34] J.J. Schröder, N. Vuxuan, Homogeneous non-equilibrium two-phase critical flow model, Chem. Eng. Technol. 10 (1987) 420–426.
[35] Y.Q. Ruan, On Entropy Balance Analyses of Non-Equilibrium Two-Phase Flow Models for Thermal-Hydraulic Computer Simulation PhD Thesis, Technical University of Munich, Munich, 1996.
[36] S.Y. Lee, V.E. Schrock, Homogeneous non-equilibrium critical flow model for liquid stagnation states, in: H.R. Jacobs (Ed.), ASME Proceedings of the 1988 National Heat Transfer Conference, ASME HTD, 1998, pp. 507–513.
[37] O.C. Jones Jr., Flashing inception in flowing liquids, ASME J. Heat Transf. 102 (1980) 439–444.
[38] C.N. Amos, V.E. Schrock, Critical discharge of initially subcooled water through slits. [PWR; BWR], United States, 1983, http://dx.doi.org/10.2172/5567881.
[39] S.Y. Lee, V.E. Schrock, Critical two-phase flow in pipes for subcooled stagnation states with a cavity flooding incipient flashing model, ASME J. Heat Transf. 112 (1990) 1033–1040.
[40] S. Levy, D. Abdollahian, Homogeneous non-equilibrium critical flow model, Int. J. Heat Mass Transf. 25 (1982) 759–770.
[41] M. Reocreux, Contribution a l'etude des debits critiques en ecoulement diphasique eauvapeur Ph.D. thesis, Université Scientifique et Medicale de Grenoble, France, 1974.
[42] B.J.C. Wu, G.A. Zimmer, Pressure and void distributions in a converging-diverging nozzle with nonequilibrium water vapor generation:: Informal Report, Technical Report, Band 26003 von BNL: Brookhaven National Laboratory, 1979. <https://books.google.de/books?id=7DnZPgAACAAJ>.
[43] J. Barták, A study of the rapid depressurization of hot water and the dynamics of vapour bubble generation in superheated water, Int. J. Multiph. Flow 16 (1990) 789–798.
[44] I. Tiselj, S. Petelin, Modelling of the critical flashing flow in the nozzle with RELAPS equations, Annual Meeting of the Nuclear Society of Slovenia, Rogaska Slatina, Slovenia, 18.–21. September, 1994.
[45] E. Elias, P.L. Chambré, Flashing inception in water during rapid decompression, ASME J. Heat Transf. 115 (1993) 231–238.
[46] V.P. Skripov, Metastable Liquids, Halsted Press, John Wiley & Sons, New York, 1974.
[47] E. Valero, I.E. Parra, The role of thermal disequilibrium in critical two-phase flow, Int. J. Multiph. Flow 28 (2002) 21–50.
[48] U. Rohatgi, E. Reshotko, Non-equilibrium one-dimensional two-phase flow in variable area channels, Proceedings of the Winter Annual Meeting, Houston, Tex., November 30–December 5, 1975.
[49] E. Elias, P.L. Chambré, Bubble transport in flashing flow, Int. J. Multiph. Flow 26 (2000) 191–206.
[50] K.H. Ardron, A two-fluid model for critical vapour-liquid flow, Int. J. Multiph. Flow 4 (1978) 323–337.
[51] M. Blander, J.L. Katz, Bubble nucleation in liquids, AIChE J. 21 (1975) 833–848.
[52] Y. Kagan, The kinetics of boiling of a pure liquid, Russ. J. Phys. Chem. 34 (1960) 42–46.
[53] W. Ruengphrathuengsuka, Bubble Nucleation and Growth Dynamics in Polymer Melts, Ph.D. thesis, Texas A & M University, 1992.
[54] P.G. Debenedetti, Metastable Liquids: Concepts and Principles, Princeton University Press, Princeton, 1996.
[55] J.R. Riznic, M. Ishii, N. Afgan, Mechanistic model for void distribution in flashing flow, Proceedings of Transient Phenomena in Multiphase Flow, ICHMT Seminar, Dubrovnik, Yugoslavia, May 24–30, 1987.
[56] E.Yu. Kumzerova, A.A. Schmidt, Effect of bubble nucleation mechanisms on flashing flow structure: numerical simulation, Comput. Fluid Dyn. J. 11 (2003) 507–512.
[57] P. Deligiannis, J.W. Cleaver, The role of nucleation in the initial phases of a rapid depressurization of a subcooled liquid, Int. J. Multiph. Flow 16 (1990) 975–984.
[58] C.A. Marsh, A.P. O'Mahony, Three-dimensional modelling of industrial flashing flows, Proceedings of CFD2008, Trondheim, Norway, 10–12 June, 2008.
[59] S.Y. Lee, Two-phase interfacial area and flow regime modelling in FLOWTRAN-TF CODE (U), Proceedings of the 1993 National Heat Transfer Conference, Atlanta, GA, August 8–11, 1993.
[60] H.M. Kottowski, Nucleation and superheating effects on activation energy of nucleation, Prog. Heat Mass Transf. 7 (1973) 299–324.
[61] R. Cole, Boiling nucleation, Adv. Heat Transf. 10 (1974) 85–166.
[62] M. Jakob, Heat Transfer, first ed., Wiley, New York, 1949.
[63] S.G. Bankoff, Entrapment of gas in spreading of a liquid over a rough surface, AIChE J. 4 (1958) 24–26.
[64] B.B. Mikić, W.M. Rohsenow, A new correlation of pool-boiling data including the effect of heating surface characteristics, ASME J. Heat Transf. 91 (1969) 245–250.
[65] K. Cornwell, R.D. Brown, Boiling surface topography, Proceedings of the 6th International Heat Transfer Conference, v. 1: Mixed Convection; Pool Boiling; Flow Boiling and Two Phase Flow, Toronto, 1978, pp. 157–161.
[66] G. Kocamustafaogullari, M. Ishii, Interfacial area and nucleation site density in boiling systems, Int. J. Heat Mass Transf. 26 (1983) 1377–1387.
[67] C.H. Wang, V.K. Dhir, Effect of surf ace wettability on active nucleation site density during pool boiling of water on a vertical surface, ASME J. Heat Transf. 115 (1993) 659–669.
[68] N. Basu, G.R. Warrier, V.K. Dhir, Onset of nucleate boiling and active nucleation site density during subcooled flow boiling, ASME J. Heat Transf. 124 (2002) 717–728.
[69] N.I. Kolev, Multiphase Flow Dynamics 2 – Thermal and Mechanical Interactions, 2nd Edition, ISBN 3-540-22107-7, Springer, Berlin Heidelberg, New York, 2005.
[70] T.S. Shin, O.C. Jones, Nucleation and flashing in nozzles-1: a distributed nucleation model, Int. J. Multiph. Flow 19 (1993) 943–964.
[71] N. Abuaf, B.J.C. Wu, G.A. Zimmer, P. Saha, A study of nonequilibrium flashing of water in a converging-diverging nozzle: Volume 1 – Experimental, U.S. Nuclear Regulatory Commission, Washington, D. C., 1981.
[72] C. Yang, Y. Wu, X. Yuan, C. Ma, Study on bubble dynamics for pool nucleate boiling, Int. J. Heat Mass Transf. 43 (2000) 203–208.
[73] N. Zuber, Flow excursions and oscillations in boiling two-phase systems with heat addition, Proceedings of EURATOM Symposium on Two-Phase Flow Dynamics, Vol. 1, pp. 1070–1089, Commission of European Communities, Brussels, 1967.
[74] O.C. Jones Jr., T.S. Shin, Flashing of initially subcooled liquid in nozzles, Presented at the 1984 Japan-U.S. Seminar on Two-phase Flow Dynamics, Lake Placid, New York, 1984.
[75] V.N. Blinkov, O.C. Jones Jr., B.I. Nigmatulin, Nucleation and flashing in nozzles – 2, Int. J. Multiph. Flow 19 (1993) 965–986.
[76] S. Maksic, D. Mewes, CFD-calculation of the flashing flow in pipes and nozzles, Proceedings of ASME FEDSM'02, Montreal, Quebec, Canada, 14–18 July, 2002.
[77] S. Mimouni, M. Boucker, J. Laviéville, A. Guelfi, D. Bestion, Modelling and computation of cavitation and boiling bubbly flows with the NEPTUNE_CFD code, Nucl. Eng. Des. 238 (2008) 680–692.
[78] J.P. Janet, Y. Liao, D. Lucas, Heterogeneous nucleation in CFD simulation of flashing flows in converging-diverging nozzles, Int. J. Multiph. Flow 74 (2015) 106–117.
[79] M.S. Plesset, S.A. Zwick, The growth of vapor bubbles in superheated liquids, J. Appl. Phys. 25 (1954) 493–500.
[80] H.K. Forster, N. Zuber, Growth of a vapor bubble in superheated liquid, J. Appl. Phys. 25 (1954) 493–500.
[81] L.E. Scriven, On the dynamics of phase growth, Chem. Eng. Sci. 10 (1959) 1–13.
[82] A.A. Avdeev, Laws of vapor bubble growth in the superheated liquid volume (thermal growth scheme), High Temp. 52 (4) (2014) 588–602.
[83] P. Dergarabedian, C. Pasadena, The rate of growth of vapor bubbles in superheated water, J. Appl. Mech. 20 (1953) 537–545.
[84] B.B. Mikić, W.M. Rohsenow, P. Griffith, On bubble growth rates, Int. J. Heat Mass Transf. 13 (1970) 657–666.
[85] Y. Zhang, X.W. Luo, B. Ji, S.H. Liu, Y.L. Wu, H.Y. Xu, A thermodynamic cavitation model for cavitating flow simulation in a wide range of water temperatures, Chin. Phys. Lett. 27 (1) (2010), 016401/1–016401/4.
[86] G.B. Wallis, Critical two-phase flow, Int. J. Multiph. Flow 6 (1980) 97–112.
[87] Y.A. Aleksandrov, Bubble Chambers, Indiana University Press, 1967.
[88] H. Kato, H. Kayano, Y. Kageyama, A consideration of thermal effects on cavitation bubble growth, ASME Proceedings: Cavitation and Multiphase Flow, 1994, pp. 7–14.
[89] Y. Utturkar, Computational Modelling of Thermodynamic Effects in Cryogenic Cavitation, PhD Thesis, The Graduate School of the University of Florida, 2005.
[90] C.E. Brennen, Cavitation and Bubble Dynamics, Oxford University Press, ISBN 0-19-509409-3, 1995.
[91] J.W. Holl, M.L. Billet, S.S. Weir, Thermodynamic effects on developed cavitation, ASME J. Fluids Eng. 97 (1975) 507–516.
[92] M.L. Billet, J.W. Holl, S.S. Weir, Correlations of thermodynamic effects for developed cavitation, ASME J. Fluids Eng. 103 (1981) 534–542.
[93] M. Deshpande, J. Feng, C.L. Merkle, Numerical modelling of the thermodynamic effects of cavitation, ASME J. Fluids Eng. 119 (1997) 420–427.
[94] T. Tokumasu, K. Kamijo, Y. Matsumoto, A numerical study of thermodynamic effects of sheet cavitation, ASME Proceedings: Cavitation and Multiphase Flow, 2002, pp. 377–382.
[95] S. Watanabe, A. Furukawa, Y. Yoshida, Theoretical analysis of thermodynamic effect of cavitation in cryogenic inducer using singularity method, Int. J. Rotating Mach. 2008 (2008) (2008) 1–8, http://dx.doi.org/10.1155/2008/125678.
[96] D.M. Liu, S.H. Liu, Y.L. Wu, H.Y. Xu, A thermodynamic cavitation model applicable to high temperature flow, Therm. Sci. 15 (2011) S95–S101.
[97] Z. Bilicki, J. Kestin, Physical aspects of the relaxation model in two-phase flow, Proc. Roy. Soc. London: Ser. A: Math., Phys. Eng. Sci. 428 (1990) 379–397.

[98] E. Faucher, J.M. Herardc, M. Barret, C. Toulemonde, Computation of flashing flows in variable cross-section ducts, Int. J. Comput. Fluid Dyn. 13 (2000) 365–391.
[99] W. Angielczyk, Y. Bartosiewicz, D. Butrymowicz, J.M. Seynhaeve, 1-D modelling of supersonic carbon dioxide two-phase flow through ejector motive nozzle, International Refrigeration and Air Conditioning Conference, Purdue, July 12–15, 2010.
[100] S. Gopalakrishnan, D.P. Schmidt, Multidimensional simulation of flash-boiling fuels in injector nozzles, 21st Annual Conference on Liquid Atomization and Spray Systems, Orlando, Florida, May 2008.
[101] K.D. Neroorkar, Modelling of Flash Boiling Flows in Injectors with Gasoline-Ethanol Fuel Blends, PhD Thesis, University of Massachusetts – Amherst, 2011.
[102] T. Ramcke, M. Pfitzner, Numerical simulation of flash evaporation in injection nozzles, ILASS Europe, 26th Annual Conference on Atomization and Spray Systems, Bremen, 2014.
[103] P. Downar-Zapolski, Z. Bilicki, L. Bolle, J. Franco, The non-equilibrium relaxation model for one-dimensional flashing liquid flow, Int. J. Multiph. Flow 22 (1996) 473–483.
[104] S. Banerjee, A surface renewal model for interfacial heat and mass transfer in transient two-phase flow, Int. J. Multiph. Flow 4 (1978) 571–573.
[105] D.A. Labuntzov, B.A. Kolchugin, V.S. Golovin, E.A. Zakharova, L.N. Vladimirova, High-speed camera investigation of bubble growth for saturated water boiling in a wide range of pressure variations, Thermophys. High Temp. 2 (1964) 446–453.
[106] W.E. Ranz, W.R. Marshall, Evaporation from drops, Chem. Eng. Prog. 48 (Part I) (1952) 141–146, Part II: 173–180.
[107] E. Ruckenstein, On heat transfer between vapour bubbles in motion and the boiling liquid from which they are generated, Chem. Eng. Sci. 10 (1959) 22–30.
[108] C.F. Schwellnus, M. Shoukri, A two-fluid model for non-equilibrium two-phase critical discharge, Can. J. Chem. Eng. 69 (1991) 188–197.
[109] Y. Liao, D. Lucas, E. Krepper, R. Rzehak, Assessment of CFD predictive capacity for flash boiling, CFD4NRS-5, Zurich, Switzerland, 9 Sep 2014.
[110] P. Saha, N. Abuaf, B.J.C. Wu, A nonequilibrium vapor generation model for flashing flows, ASME J. Heat Transf. 106 (1984) 198–203.
[111] D.L. Chang, C.F. Lee, Preliminary computational studies of flash boiling for fuel injectors in Gasoline direct injection automotive engines, Proceedings of 3th Intersociety Energy Conversion Engineering Conference (IECEC), 2002, pp. 464–469.
[112] T. Hibiki, M. Ishii, Active nucleation site density in boiling systems, Int. J. Heat Mass Transf. 46 (2003) 2587–2601.
[113] C.A. Marsh, A.P. O'Mahony, Three-dimensional modelling of industrial flashing flows, Prog. Comput. Fluid Dyn. 9 (2009) 393–398.
[114] Th. Frank, P.J. Zwart, E. Krepper, H.-M. Prasser, D. Lucas, Validation of CFD models for mono- and polydipserse air-water two-phase flows in pipes, Nucl. Eng. Des. 238 (2008) 647–659.
[115] S. Hänsch, D. Lucas, E. Krepper, T. Höhne, A multi-field two-fluid concept for transitions between different scales of interfacial structures, Int. J. Multiph. Flow 47 (2012) 171–182.
[116] E.S. Starkman, V.E. Schrock, K.F. Neusen, D.J. Maneely, Expansion of a very low quality two-phase fluid through a convergent-divergent nozzle, ASME J. Basic Eng. 86 (2) (1964) 247–255.
[117] J.C. Leung, A generalized correlation for one-component homogeneous equilibrium flashing choked flow, AIChE J. 32 (1986) 1743–1746.
[118] J.C. Leung, M.A. Grolmes, The discharge of two-phase flashing flow in a horizontal duct, AIChE J. 33 (1987) 524–527.
[119] J.C. Leung, Similarity between flashing and nonflashing two-phase flows, AIChE J. 36 (1990) 797–800.
[120] J.C. Leung, The Omega Method for Discharge Rate Evaluation, International Symposium on Runaway Reactions and Pressure Relief Design, Boston, 1995.
[121] F. Inada, T. Ohkawa, Thermo-hydraulic instability of natural circulation BWRs (Explanation on instability mechanisms at start-up by homogeneous and thermo-dynamic equilibrium model considering flashing effect), Proceedings of International Conference on New Trends in Nuclear System Thermohydraulics (1994) 187–193.
[122] D.D.B. Van Bragt, W.J.M. De Kruijf, A. Manera, T.H.J.J. Van Der Hagen, H. Van Dam, Analytical modelling of flashing-induced instabilities in a natural circulation cooled boiling water reactor, Nucl. Eng. Des. 215 (2002) 87–98.
[123] F.J. Moody, Maximum flow rate of a single component. Two-phase mixture, ASME J. Heat Transf. 87 (1965) 134–141.
[124] F.J. Moody, Maximum two-phase vessel blowdown from pipes, ASME J. Heat Transf. 88 (1966) 285–294.
[125] H. K. Fauske, Two-phase critical flow with application to liquid-metal systems (Mercury, Cesium, Rubidium, Potassium, Sodium, and Lithium), Technical report, ANL-6633, 1963.
[126] S. Levy, Steam slip – theoretical prediction from momentum model, ASME J. Heat Transf. 82 (1960) 113–124.
[127] S. Levy, Prediction of two-phase critical flow rate, ASME J. Heat Transf. 87 (1) (1965) 53–57.
[128] S.Y. Ahmad, Axial distribution of bulk temperature and void fraction in a heated channel with inlet subcooling, ASME J. Heat Transf. 92 (1970) 595–609.
[129] E. Elias, P.L. Chambré, A mechanistic non-equilibrium model for two-phase critical flow, Int. J. Multiph. Flow 10 (1) (1984) 21–40.
[130] D.P. Schmidt, C.J. Rutland, M.L. Corradini, A fully compressible model of cavitating flow, Atomization Sprays 9 (1999) 255–276.
[131] S. Gopalakrishnan, Modelling of Thermal Non-Equilibrium in Superheated Injectors Flows, PhD Thesis, University of Massachusetts – Amherst, 2010.
[132] J. Riznic, M. Ishii, Bubble number density in vapor generation and flashing flow, Int. J. Heat Mass Transf. 32 (1989) 1821–1833.
[133] M. Wein, J. Huhn, Numerical simulation of non-equilibrium hot-water two-phase flows, Convective Flow and Pool Boiling Conference, Kloster Irsee, Germany, 1997.
[134] F. Inada, M. Furuya, A. Yasuo, Thermo-hydraulic instability of boiling natural circulation loop induced by flashing (analytical consideration, Nucl. Eng. Des. 2000 (2000) 187–199.
[135] A. Manera, Out-of-Phase flashing-induced instabilities in natural circulation two-phase system with parallel channels, 4th International Conference on Transport Phenomena in Multiphase Systems (HEAT2005), Gdańsk, Poland, June 26–30, 2005.
[136] A. Manera, Strategies for the start-up procedure of natural circulation boiling water reactors, Jahrestagung Kerntechnik 2005, Nürnberg, Germany, May 10–12, 2005.
[137] A. Manera, A startup procedure for natural circulation boiling water reactors, The 11th International Topical Meeting on Nuclear Reactor Thermal-Hydraulics (NURETH-11), Popes' Palace Conference Center, Avignon, France, October 2–6, 2005.
[138] A. Manera, U. Rohde, H.-M. Prasser, T.H.J.J. van der Hagen, Modelling of flashing-induced instabilities in the start-up phase of natural-circulation BWRs using the two-phase flow code FLOCAL, Nucl. Eng. Des. 235 (2005) 1517–1535.
[139] F. Schäfer, A. Manera, Investigation of flashing-induced instabilities at the CIRCUS test facility using the code ATHLET, 10th International Topical Meeting on Nuclear Reactor Thermal Hydraulics (NURETH-10), Seoul, Korea, October 5–9, 2003.
[140] F. Schäfer, A. Manera, Investigation of flashing-induced instabilities at CIRCUS test facility with the code ATHLET, Int. J. Nucl. Energy Sci. Technol. 2 (2006) 209–218.
[141] G. Yadigaroglu, B. Askari, Boiling water reactor stability revisited: the effects of flashing, Nucl. Eng. Des. 235 (2005) 1093–1105.
[142] M. Furuya, F. Inada, T.H.J.J. van der Hagen, Flashing-induced density wave oscillations in a natural circulation BWR-mechanism of instability and stability map, Nucl. Eng. Des. 235 (2005) 1557–1569.
[143] R. Dagan, E. Elias, E. Wacholder, S. Olek, A two-fluid model for critical flashing flows in pipes, Int. J. Multiph. Flow 19 (1993) 15–25.
[144] J.L. Muñoz-Cobo, E. Cerezo, S. Chiva, Two phase flow modelling of flashing critical and noncritical flows in converging-diverging nozzles, 4th International Conference on Multiphase Flow-ICMF'2001, New Orleans, May 27, 2001.
[145] M. Wein, Numerische Simulation on kritischen und nahkritische Zweiphasenströmungen mit thermischen und fluiddynamischen Nichtgleichgewichtseffekten, PhD Thesis, Dresden University of Technology, 2002.
[146] T. Giese, E. Laurien, A thermal based model for cavitation in saturated liquids, Zeitschrift für angewandte Mathematik und Mechanik 81 (2001) 957–958.
[147] J. Kutnjak, R. Kulenovic, E. Laurien, Experimental investigation and modelling of bulk boiling for CFD application, The 14th International Topical Meeting on Nuclear Reactor Thermal hydraulics, NURETH-14, Toronto, Ontario, Canada, September 25–30, 2011.
[148] C. Marsh, D. Withers, CFD modelling of direct contact steam injection, Fifth International Conference on CFD in the Process Industries, CSIRO, Melbourne, Australia, 13–15 December, 2006.
[149] E. Laurien, T. Giese, Exploration of the two fluid model of two-phase flow towards boiling, cavitation and stratification, The 3rd International Conference on Computational Heat and Mass Transfer, Banff, Canada, May 26–30, 2003.
[150] T. Xing, S.H. Frankel, Effect of cavitation on vortex dynamics in a submerged laminar jet, AIAA J. 40 (11) (2002) 2266–2276.
[151] G. Palau-Salvador, P. González-Altozano, J. Arviza-Valverde, Numerical modelling of cavitating flows for simple geometries using FLUENT V6.1, Spanish J. Agric. Res. 5 (2007) 460–469.
[152] M. Ishigaki, T. Watanabe, H. Nakamura, Numerical simulation of two-phase critical flow with the phase change in the nozzle tube, J. Power Energy Syst. 6 (2012) 264–274.
[153] J. Yang, O.C. Jones Jr., T.S. Shin, Critical flow of initially subcooled flashing liquids: limitations in the homogeneous equilibrium model, Nucl. Eng. Des. 95 (1986) 197–206.
[154] R.E. Henry, The two-phase critical discharge of initially saturated or subcooled liquid, Nucl. Sci. Eng. 41 (1970) 336–342.
[155] R.E. Henry, H.K. Fauske, The two-phase critical flow of one-component mixtures in nozzles, orifices and tubes, ASME J. Heat Transf. 93 (1971) 179–187.
[156] C. Lackmé, Thermodynamics of critical two-phase discharge from long pipes of initially subcooled water, ICHMT Digit. Libr. 1982 (1982) 391–407.
[157] M. Ishii, One-dimensional drift-flux model and constitutive equations for relative motion between phases in various two-phase flow regimes, Argonne National Laboratory, USA, ANL-77-47, 1977.
[158] N. Zuber, J.A. Findlay, Average volumetric concentration in two-phase flow system, ASME J. Heat Transf. 87 (1965) 453–468.

[159] IAEA, Thermal-hydraulic relationships for advanced water cooled reactors, IAEA-TECDOC-1203, 2001.
[160] J.T. Kuo, G.B. Wallis, H.J. Richter, Interphase momentum transfer in the flow of bubbles through nozzles. Topical Report, EPRI, NP-980, 1979.
[161] H.J. Richter, S.E. Minas, Separated two-phase flow model for critical two-phase flow, Proceedings of Non-Equilibrium Interfacial Transport Processes, ASME Meeting, San Diego, 1979.
[162] H.J. Richter, Separated two-phase flow: application to critical two-phase flow, EPRI, NP-1800, 1981.
[163] O.C. Jones Jr., N. Zuber, Bubble growth in variable pressure fields, ASME J. Heat Transf. 100 (1978) 453–459.
[164] T.S. Shin, O.C. Jones Jr., An active cavity model for flashing, Nucl. Eng. Des. 95 (1986) 185–196.
[165] Ansys, C. Release 14.5. ANSYS CFX-Solver Theory Guide. ANSYS, 2012.
[166] Y. Liao, D. Lucas, Possibilities and limitations of CFD simulation for flashing flow scenarios in nuclear applications, Energies 10 (139) (2017), http://dx.doi.org/10.3390/en10010139.
[167] Y. Liao, R. Rzehak, D. Lucas, E. Krepper, Baseline closure model for dispersed bubbly flow: bubble coalescence and breakup, Chem. Eng. Sci. 122 (2015) 336–349.